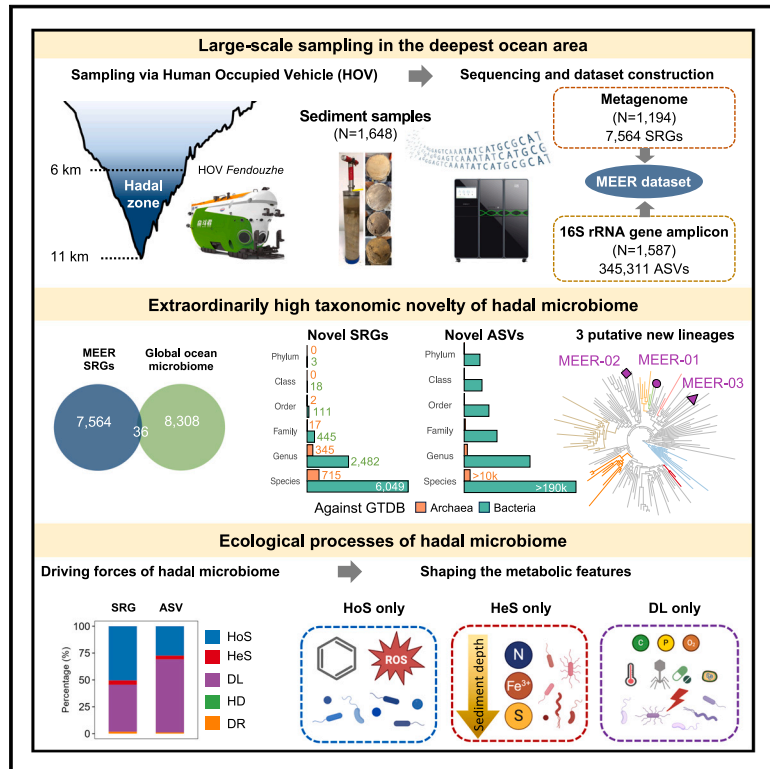


Microbial ecosystems and ecological driving forces in the deepest ocean sediments

Graphical abstract



Authors

Xiang Xiao, Weishu Zhao, Zewei Song, ..., Mo Han, Xun Xu, Shanshan Liu

Correspondence

zjxiao2018@sjtu.edu.cn (X.X.),
zwsh88@sjtu.edu.cn (W.Z.),
wzhang@idsse.ac.cn (W.-J.Z.),
hanmo@genomics.cn (M.H.),
xuxun@genomics.cn (X.X.),
liushanshan@mgi-tech.com (S.L.)

In brief

Metagenomic sequencing of 1,648 sediment samples from 6–11 km water depths, including the Mariana Trench, highlights the hadal microbial ecosystem and its environmental driving forces.

Highlights

- Large-scale investigation of hadal sediments generated the MEER microbial dataset
- Reveals extraordinarily high proportion of unidentified microbial taxa in hadal zone
- Identify two hadal microbial adaptation strategies: streamlined and versatile
- Aromatic compound utilization and antioxidation emerge as key adaptations to hadal zone



Article

Microbial ecosystems and ecological driving forces in the deepest ocean sediments

Xiang Xiao,^{1,26,27,*} Weishu Zhao,^{1,26,*} Zewei Song,^{2,9,15,26} Qi Qi,^{1,26} Bo Wang,^{3,15,26} Jiahui Zhu,^{2,9,26} James Lin,^{10,26} Jing Wang,^{1,7,25,26} Aoran Hu,^{1,26} Shanshan Huang,^{1,25,26} Yinzhao Wang,¹ Jianwei Chen,^{4,11,12} Chao Fang,^{9,15} Qianyue Ji,⁴ Nannan Zhang,⁴ Liang Meng,⁴ Xiaofeng Wei,^{3,18} Chuanxu Chen,⁵ Shanya Cai,⁵ Shun Chen,⁵ Kang Ding,⁵ Dong Li,⁵

(Author list continued on next page)

¹State Key Laboratory of Microbial Metabolism, International Center for Deep Life Investigation (IC-DLI), School of Life Sciences and Biotechnology, Shanghai Jiao Tong University, Shanghai 200240, China

²BGI Research, Sanya 572025, China

³China National GeneBank, BGI Research, Shenzhen 518083, China

⁴BGI Research, Qingdao 266555, China

⁵Institute of Deep-sea Science and Engineering, Chinese Academy of Sciences, Sanya, China

⁶College of Marine Science and Technology, Hainan Tropical Ocean University, Sanya 572000, China

⁷School of Oceanography, Shanghai Jiao Tong University, Shanghai, China

⁸MGI Tech, Shenzhen 518083, China

⁹BGI Research, Shenzhen 518083, China

¹⁰Center for High Performance Computing, Shanghai Jiao Tong University, Shanghai, China

¹¹Institute of Metagenomics, Qingdao-Europe Advance Institute for Life Sciences, BGI Research, Qingdao 266555, China

¹²Laboratory of Genomics and Molecular Biomedicine, Department of Biology, University of Copenhagen, 2100 Copenhagen, Denmark

¹³BGI, Shenzhen 518083, China

¹⁴Guangdong Provincial Key Laboratory of Genome Read and Write, BGI Research, Shenzhen 518083, China

¹⁵Shenzhen Key Laboratory of Environmental Microbial Genomics and Application, BGI Research, Shenzhen 518083, China

¹⁶Shenzhen Key Laboratory of Marine Genomics, BGI Research, Shenzhen 518083, China

¹⁷Institution of Deep-Sea Life Sciences, IDSSE-BGI, Hainan Deep-sea Technology Laboratory, Sanya, Hainan, China

¹⁸Genomics Data Center of Guangdong Province, BGI Research, Shenzhen 518083, China

¹⁹Institute of Environment and Ecology, Tsinghua Shenzhen International Graduate School, Tsinghua University, Shenzhen 518055, China

²⁰Institute for Environmental Genomics, University of Oklahoma, Norman, OK 73019, USA

²¹School of Biological Sciences, University of Oklahoma, Norman, OK 73019, USA

²²School of Civil Engineering and Environmental Sciences, University of Oklahoma, Norman, OK 73019, USA

²³School of Computer Sciences, University of Oklahoma, Norman, OK 73019, USA

²⁴Earth and Environmental Sciences, Lawrence Berkeley National Laboratory, Berkeley, CA 94720, USA

²⁵Shanghai Jiao Tong University Hainan Research Institute, Sanya 572025, China

(Affiliations continued on next page)

SUMMARY

Systematic exploration of the hadal zone, Earth's deepest oceanic realm, has historically faced technical limitations. Here, we collected 1,648 sediment samples at 6–11 km in the Mariana Trench, Yap Trench, and Philippine Basin for the Mariana Trench Environment and Ecology Research (MEER) project. Metagenomic and 16S rRNA gene amplicon sequencing generated the 92-Tbp MEER dataset, comprising 7,564 species (89.4% unreported), indicating high taxonomic novelty. Unlike in reported environments, neutral drift played a minimal role, while homogeneous selection (HoS, 50.5%) and dispersal limitation (DL, 43.8%) emerged as dominant ecological drivers. HoS favored streamlined genomes with key functions for hadal adaptation, e.g., aromatic compound utilization (oligotrophic adaptation) and antioxidation (high-pressure adaptation). Conversely, DL promoted versatile metabolism with larger genomes. These findings indicated that environmental factors drive the high taxonomic novelty in the hadal zone, advancing our understanding of the ecological mechanisms governing microbial ecosystems in such an extreme oceanic environment.

INTRODUCTION

The hadal zone, defined as oceanic regions exceeding 6 km below sea level (b.s.l.) and reaching approximately 11 km at

the Challenger Deep in the Mariana Trench (MT), represents one of Earth's most inaccessible and least explored environments.^{1–3} This extreme environment is characterized by immense hydrostatic pressure, which increases linearly with



Shuangquan Liu,⁵ Taoran Song,⁶ Liyang Tian,⁵ Haibin Zhang,^{5,17} Yu Zhang,⁷ Shiyu Xu,⁸ Jiayu Chen,³ Haixin Chen,² Qian Cen,³ Fangfang Jiang,³ Guohai Hu,^{3,15} Chenguang Tang,⁸ Wu Guo,¹⁰ Xiaohan Wang,⁹ Liping Zhan,⁴ Jie Fan,⁴ Jun Wang,² Changhao Zhou,⁴ Liuyang Li,¹ Zhenbo Lv,¹ Yaoxun Hu,¹ Xiaonan Lin,² Guoqiang Mai,³ Linlin Luo,³ Tao Yang,^{3,13} Weiwen Wang,^{3,13} Karsten Kristiansen,^{9,11,12} Liqun Chen,³ Huanming Yang,¹³ Ming Ni,⁸ Ying Gu,⁹ Feng Mu,⁸ Yunfeng Yang,¹⁹ Jizhong Zhou,^{20,21,22,23,24} Jian Wang,¹³ Wei-Jia Zhang,^{5,17,*} Mo Han,^{2,9,12,15,*} Xun Xu,^{9,14,*} and Shanshan Liu^{4,8,16,17,*}

²⁶These authors contributed equally

²⁷Lead contact

*Correspondence: zjxiao2018@sjtu.edu.cn (X.X.), zwsh88@sjtu.edu.cn (W.Z.), wzhang@idsse.ac.cn (W.-J.Z.), hanmo@genomics.cn (M.H.), xuxun@genomics.cn (X.X.), liushanshan@mgi-tech.com (S.L.)

<https://doi.org/10.1016/j.cell.2024.12.036>

water depth, ranging from 60 to 115 MPa in the hadal zone.⁴ The extreme pressure characteristic of hadal environments has long posed significant challenges for systematic investigations and sample collection in these deep-sea ecosystems. Using the MT as a representative system, previous metagenomic studies of hadal sediment microbiomes have been limited to 96 samples from 34 sampling sites across nine publications, typically examining only 1–3 sampling sites per study with an average sequencing of 12.1 giga base pairs (Gbps) per sample.^{5–13}

Beyond technical accessibility, the hadal zone presents extraordinary environmental challenges to life, combining extreme hydrostatic pressure, near-freezing temperatures, and oligotrophic conditions—a unique combination that sets it apart from all other marine and terrestrial environments.^{1,14,15} Despite the sampling constraints, preliminary research has revealed intriguing evidence suggesting that hadal microorganisms differ substantially from their counterparts in upper ocean layers,^{11,16} as well as distinctions between microbiomes at trench bottom and on slopes.¹⁰ Prior studies have attributed microbial community variations to the heterogeneous distribution of organic matter and distinct redox stratification in hadal sediments—featuring oxic, nitrogenous, and ferruginous zones—which markedly differ from abyssal plain sediments.¹⁷ However, how the harsh hadal conditions, especially the extreme high pressure, shape the hadal microorganisms and their communities remains unclear, due to the scarcity of samples and limited spatial coverage.

Recent studies suggested previously unreported hadal microbiomes at the species level,^{5,11} although the main phyla in hadal zone were similar to the other places in ocean area, including Pseudomonadota, Chloroflexota, and Marinisomatota as typical bacterial phyla, and Nanoarchaeota, Thermoplasmatota, and Thermoproteota as typical archaeal phyla.^{9,10,12} Importantly, representative hadal microorganisms exhibit diverse phylogenetic and adaptation patterns. For instance, ammonia-oxidizing archaea (AOA) Nitrososphaerota (belonging to Thermoproteota, previously known as Thaumarchaeota) displays distinct phylotype shifts between hadal and shallow-water clades while maintaining ammonia-oxidizing functionality.¹⁸ By contrast, hadal Chloroflexota and anammox bacteria Brocadiales (belonging to Planctomycetota) remain phylogenetically close to their shallow-water relatives but have evolved piezotolerance and metabolic versatility.^{5,19} The experimental constraints of hadal environments have limited our mechanistic understanding of these divergent adaptations. However, well-established ecological theories offer powerful frameworks for decoding microbial adaptation in these extreme depths.

Microbial ecologists have developed methodologies to decipher community-driving forces, primarily utilizing 16S rRNA gene amplicon sequencing.^{20–22} The iCAMP framework,²³ for instance, dissects five primary ecological drivers: homogeneous selection (HoS), heterogeneous selection (HeS), dispersal limitation (DL), homogenizing dispersal (HD), and drift (DR). DR embodies neutral evolution,²⁴ while the other four processes relate to macro- and microenvironmental impacts. Specifically, natural selection processes manifest in two forms: HoS, where similar environments select for similar ecological niches, and HeS, where distinct environments favor different niches.^{25,26} Beyond natural selection, environmental influences are also evident in DL and HD, which reflect the restricted microbial spreading and free dispersal, respectively.^{25,26}

Disentangling ecological processes can elucidate environmental influences on microbial communities, yet applying these analyses to hadal environments presents significant challenges. Firstly, robust ecological studies typically require a substantial sample size (tens to hundreds) to yield meaningful conclusions,²⁷ necessitating the overcoming of technical limitations in hadal sampling. Secondly, conventional ecological approaches based on 16S rRNA gene amplicon sequencing left the gap between taxonomic composition and metabolic potentials, especially for the poorly explored environments such as the hadal zone.²⁸ Consequently, a comprehensive understanding of the ecological processes shaping hadal microbial ecosystems and their metabolism remains elusive.

This study aims to address the aforementioned challenges and provide a comprehensive understanding of the microbial ecosystem and its underlying driving forces in Earth's deepest oceanic environments. Here, we utilized the human-occupied vehicle (HOV) *Fendouzhe* to collect 1,648 sediment samples from the MT, Yap Trench, and Philippine Basin and performed metagenomic and 16S rRNA gene amplicon sequencing on these hadal samples. Both shotgun metagenome-derived species-level representative genomes (SRGs) and 16S rRNA gene amplicon sequence variants (ASVs) revealed exceptionally high taxonomic novelty in hadal microorganisms compared with shallower oceanic ecosystems and public databases. We developed SRG-based approaches, complemented by classical ASV-based analyses, to elucidate the spatial and vertical distributions of microbial communities and their underlying ecological processes in the hadal zone. The SRG-based ecological analysis provided a comprehensive link between community assembly, genomic features, and metabolic potentials, uncovering two distinct adaptation strategies employed by hadal microorganisms in the deepest ocean sediments.

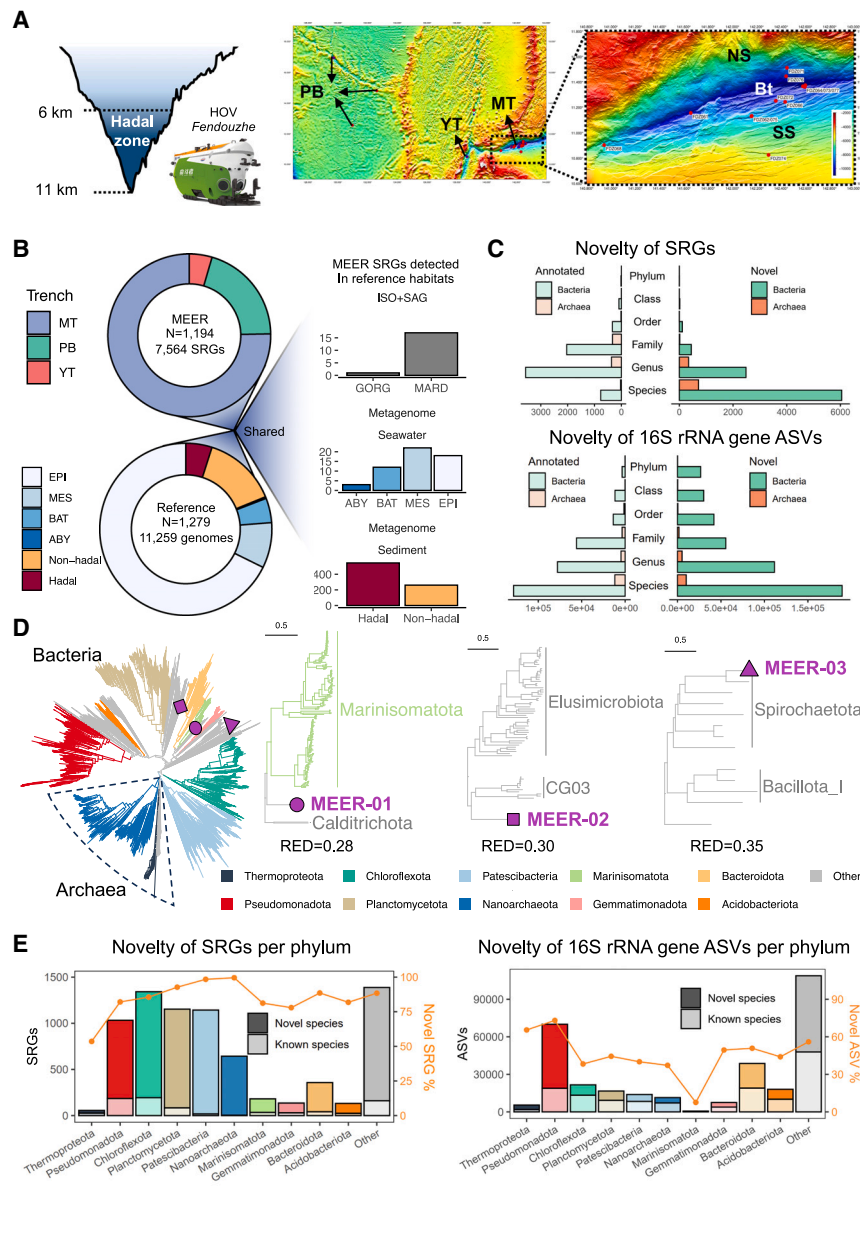


Figure 1. Sampling and extraordinary novelty of the Deepest Ocean microbiome revealed by the MEER dataset

(A) Sampling sites of hadal zones using the human-occupied vehicle (HOV) *Fendouzhe* in this study, including the Philippine Basin (PB), the Yap Trench (YT), and the Mariana Trench (MT), as well as the bottom (Bt), northern slope (NS), and southern slope (SS) within the Mariana Trench.

(B) Comparative analysis between the species-level representative genomes (SRGs) from the MEER dataset and the species-level genomes in the Ocean Microbiomics Database (OMD), the typical deep-sea and hadal sediment. The OMD included isolated reference genome (ISO) of Global Ocean Reference Genomes (GORG), single-cell amplified genome (SAG) of MAR Database (MARD), as well as seawater metagenomes of abyssopelagic layer (ABY, 4,500–6,000 m), bathypelagic layer (BAT, 1,000–4,500 m), mesopelagic layer (MES, 200–1,000 m), and epipelagic layer (EPI, 0–200 m). Doughnut charts illustrate the sample habitat distribution in each habitat. Bar plots depict the distribution of MEER SRGs detected in reference habitats.

(C) Taxonomic novelty of the MEER dataset against the Genome Taxonomy Database (GTDB, release 220). Light bars extending leftward indicate the finest taxonomic level to which SRGs or 16S rRNA gene amplicon sequence variants (ASVs) can be annotated. Solid bars extending rightward represent unreported taxa at each taxonomic level.

(D) *De novo* phylogenetic tree of SRGs, color-coded by the 10 most abundant phyla in the MEER dataset. Purple shapes indicate the placement of three bacterial SRGs that could not be assigned to known phyla according to GTDB, with subtrees showing their neighboring clades and relative evolutionary divergence (RED) values. Note that the bacterial and archaeal trees were combined for visualization purpose but were not rooted together.

(E) Distribution of novelty among SRGs and 16S rRNA gene ASVs across the 10 most abundant phyla. Stacked bar plots represent the number of unreported and known SRGs or ASVs, while orange lines and dots indicate the percentage of novelty.

See also [Figure S1](#) and [Tables S1](#) and [S2](#).

RESULTS

Systematic sampling and sequencing in the hadal zone

We conducted an extensive sediment sampling campaign using the HOV *Fendouzhe*, collecting 1,648 sediment samples from 145 sites during 32 dives across three hadal regions: the MT (1,209 samples, 6–11 km b.s.l., encompassing the Challenger Deep's bottom axis and slopes), Yap Trench (YT, 72 samples, ~9 km b.s.l.), and Philippine Basin (PB, 367 samples, 6–8 km b.s.l.) ([Figures 1A](#) and [S1](#); [Table S1](#)). This sample set, over 10-fold larger than all previously reported hadal collections, enabled the collaborative scientific team to initiate the MT Environment and Ecology (MEER) project, aiming to systematically

profile the hadal microbial ecosystem through a series of integrated investigations.

Among 1,648 hadal sediment samples, shotgun metagenomic sequencing was successfully performed on 1,194 samples, yielding an average of 77.26 ± 32.41 Gbp of paired-end 150 bp metagenomic data per sample ([STAR Methods](#)). These data generated 106,501 medium-quality or higher metagenome-assembled bins (completeness $\geq 50\%$ and contamination $\leq 10\%$).²⁹ After dereplication at 95% whole-genome average nucleotide identity (ANI), we obtained 7,564 SRGs. Additionally, 16S rRNA gene V4 region amplicon sequencing of 1,587 samples yielded 345,311 denoised nonchimeric ASVs. Collectively, these representative SRGs and ASVs constitute the MEER

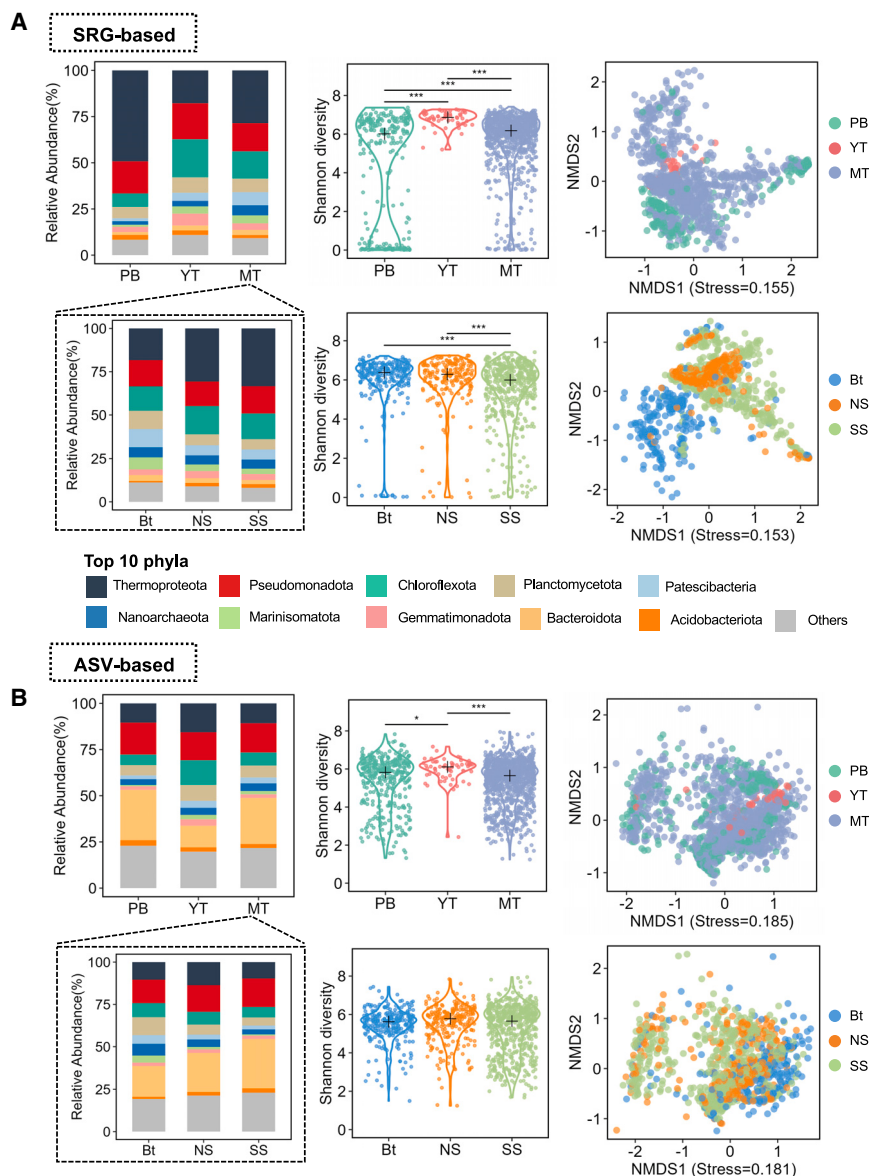


Figure 2. The spatial distribution of the microbiome in the hadal zone

(A) SRG-based microbial taxonomic composition, Shannon diversity, and non-metric multidimensional scaling (NMDS) analysis in the Philippine Basin (PB), the Yap Trench (YT), and the Mariana Trench (MT), as well as the bottom (Bt), northern slope (NS), and southern slope (SS) within the Mariana Trench.

(B) 16S rRNA gene amplicon sequence variant (ASV)-based microbial taxonomic composition, Shannon diversity, and NMDS analysis in three trenches/basins (PB, YT, and MT), as well as different topographical areas (Bt, NS, and SS) within the MT. The black cross of violin chart represented the median value. The asterisks indicated significant differences using pairwise Wilcoxon rank-sum test: *** $p < 0.001$, ** $p < 0.01$, * $p < 0.05$. See also Figure S2.

efforts have unveiled a substantial number of previously uncharacterized microbial species in the deepest ocean ecosystems.

We also compared the MEER SRGs with the latest version of the Genome Taxonomy Database (GTDB, release 220),⁴⁹ The MEER SRGs encompassed 77 bacterial and 9 archaeal phyla, with the top 10 abundant phyla accounting for 6,176 (81.6%) of the total SRGs and nearly 90.0% of the total taxonomic relative abundance among all samples (Figure 2B). Remarkably, 6,764 SRGs (89.4%) were not previously represented in the GTDB, with most phyla, including 9 of the top 10 (excluding Thermoproteota), containing over 70.0% previously unidentified SRGs (Figure 1E). Of these SRGs, 2,827 represented genera or higher taxonomic ranks (Figure 1C). Notably, three SRGs (named as MEER-

dataset, providing a comprehensive genomic and taxonomic profile of the ecosystem in the hadal zone.

Exceptional taxonomic novelty of hadal microbiome

To evaluate the novelty of the SRGs in the MEER dataset, we conducted comparative analyses with three reference datasets (Table S2): the Ocean Microbiomics Database (OMD),³⁰ a collection of typical deep-sea sediment metagenomes (2,073 species-level genomes from 178 samples),^{31–47} and previously reported hadal metagenomes (878 SRGs from 63 samples).^{5,9,10,12,13,48} At the 95% ANI threshold, the MEER dataset showed minimal overlap with these references (Figure 1B). Only 36 SRGs (0.5%) from MEER overlapped with the OMD dataset, 261 SRGs (3.5%) with typical deep-sea sediment genomes, and notably, only 545 SRGs (7.2%) with existing MT data. These results revealed that our systematic sampling and sequencing

01, MEER-02, and MEER-03) could not be assigned even at the phylum level. They exhibited relative evolutionary divergence (RED) values of 0.28, 0.30, and 0.35, respectively, from the root of the GTDB bacterial reference tree. These values fall within the range of phylum-level RED values (0.37 ± 0.1).⁵⁰ According to their distinct positions within the *de novo* phylogenetic tree (Figure 1D), these SRGs potentially represent three undocumented high-level lineages.

The 16S rRNA gene amplicon sequencing analysis corroborated the high taxonomic novelty observed in the MEER dataset. When compared with the GTDB database (release 220), 207,772 out of 345,311 ASVs (60.2%) could not be mapped to any reference 16S rRNA gene sequences at the species level 97% identity threshold (Figure 1C). Among the 10 most abundant phyla in the MEER dataset, 30%–70% of ASVs were unmapped, with the exception of Marinisomatota, which comprised 10% unmapped

species (Figure 1E). To validate our findings, we extended the comparison to other prominent 16S rRNA gene databases. Similar patterns emerged with the SILVA database (release 138)⁵¹ and Greengenes2 database (release 2022.10),⁵² where 37.6% and 56.6% of ASVs remained unmatched, respectively. These consistent results across multiple reference databases further emphasize the significant microbial novelty represented in the MEER dataset. For consistency and to facilitate direct comparison with our SRG-based analysis, we present the GTDB-based findings throughout the remainder of this manuscript.

High diversity of the microbial community across different hadal zones

The comprehensive MEER dataset provides a systematic overview to reveal both high microbial species novelty and remarkable diversity in hadal samples. Despite the hadal zone's minuscule area relative to the global ocean, its microbial diversity is remarkably comparable. The within-sample microbial diversity in MEER samples, quantified by the Shannon index, averaged 5.5 (SRG level, average mapping rate 68%) and 5.4 (ASV level), closely matching the mean of 5.8 (SRG level, average mapping rate 49%) observed in OMD samples from the global ocean. This remarkable parity demonstrates that hadal zones, despite occupying less than 1% of global ocean area,⁴ maintain microbial complexity comparable to more extensive marine ecosystems.

Between-sample diversity exhibited remarkable variation, with average Bray-Curtis dissimilarities of 0.75 (SRG level) and 0.86 (ASV level) across MT, YT, and PB. Notably, within MT alone, high average dissimilarity values persisted at 0.73 (SRG level) and 0.85 (ASV level). The SRG-based analysis generally yielded lower dissimilarity values compared with ASV-based results, likely attributable to the broader taxonomic detection range of 16S rRNA gene amplicon sequencing, which can capture taxa that are challenging to assemble into high-quality SRGs. Nevertheless, the SRG-level and ASV-level diversities were significantly correlated (mantel $r = 0.45$, $p < 0.01$), indicating that both methods capture consistent major diversity patterns in MEER samples. Additionally, these Bray-Curtis dissimilarity values are comparable to the 0.86 (SRG level) observed among OMD's global ocean samples, underscoring the exceptional diversity of microbial community structures in MEER samples. This remarkable community-level variation, both across hadal regions and within the MT, persisting despite extreme hydrostatic pressure, near-freezing temperatures, and severe nutrient limitation, demonstrates the extraordinary adaptive capacity of microbial life at Earth's greatest depths.

Across the three hadal zones, both Shannon indices and phylogenetic diversity metrics revealed congruent patterns, demonstrating significantly higher within-sample diversity in YT compared with MT and PB (Wilcoxon rank-sum test). SRG-based analyses further indicated higher Shannon indices in MT than in PB, whereas ASV-based calculations showed no significant differences between these two trenches (Figures 2A, 2B, S2A, and S2B). Within different regions of the MT (bottom, southern, and northern slope), SRG-based results revealed greater

within-sample diversity at the trench bottom compared with the slopes, suggesting a more complex microbial community in the deepest part of the trench. However, no significant differences were shown in ASV-based results (Figures 2A and 2B). These results suggest that the statistical significance and interpretability of diversity indices may vary between these two methodologies.

Nonmetric multidimensional scaling (NMDS) and principal coordinates analysis (PCoA), based on Bray-Curtis dissimilarity, revealed significantly distinct microbial community structures among PB, YT, and MT samples (PERMANOVA; $R^2 = 0.07$, $p < 0.01$ for SRGs; $R^2 = 0.02$, $p < 0.01$ for ASVs), as well as between bottom and slope samples within MT (PERMANOVA; $R^2 = 0.12$, $p < 0.01$ for SRGs; $R^2 = 0.05$, $p < 0.01$ for ASVs) (Figures 2A, 2B, S2A, and S2B). However, geological zonation only explains a small fraction of total community variations, with SRG-based results accounting for a larger proportion compared with ASV-based results, as indicated by the R^2 values in the PERMANOVA analysis. This outcome suggests that SRG-based methods may more closely represent the biogeographic distribution of the hadal microbiome, while ASV-based results might capture more local variations. The explanatory power of geological factors remains limited even when considering only surface (0–2 cm) sediment samples, with R^2 values of 0.17 (SRG-based) and 0.12 (ASV-based). These results reveal that hadal microbial diversity is significantly influenced by additional and yet-to-be-characterized factors beyond the well-acknowledged large-scale geographical zonation¹⁷ and redox gradients along sediment depth.⁵³ To decode these complex patterns, we employed detailed ecological analyses, aiming to unveil both the direct drivers of hadal microbiomes and the hidden forces governing these unique ecosystems.

Ecological processes of the microbial community in hadal sediments

The large-scale, intensive sampling in the hadal zone yielded statistically robust results and enhanced resolution for ecological analysis. We employed the iCAMP framework²³ to analyze the ecological processes shaping the microbial community, utilizing both classical 16S rRNA gene ASVs and SRGs (STAR Methods). A generally consistent trend in ecological processes of the hadal microbiome was obtained. Both 16S rRNA gene ASV- and SRGs-based analyses revealed that HoS and DL were the predominant driving forces shaping the microbial community in the hadal zone (Figure 3A).

In comparison to reported oceanic and terrestrial environments, including saline sediment,⁵⁴ coastal sediment,⁵⁵ mangrove sediment,⁵⁶ soil,^{23,57–59} and water,^{22,60–62} the hadal microbiome exhibited obviously lower percentages of DR, while HD was undetectable in the hadal zones (Figure 3A). This ecological profile indicated the distinct selective pressures of the hadal environment. Notably, previous studies using 16S rRNA gene amplicon sequencing reported that DR substantially contributed (37.4%) to microbial communities in YT sediments at shallower water depths (4,000–7,000 m).⁶³ By contrast, our MEER dataset, also employing 16S rRNA gene amplicon sequencing, revealed that in the deepest region of the YT (~9,000 m), DR accounted

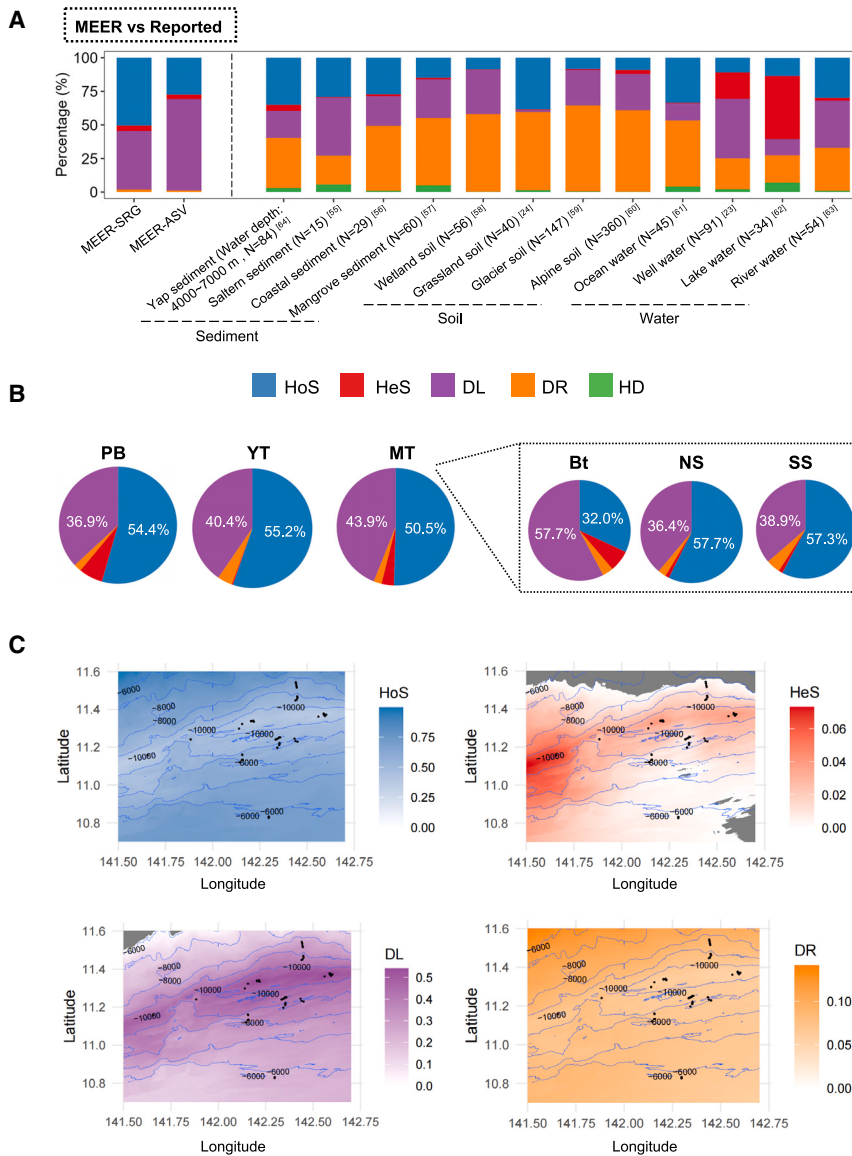


Figure 3. Ecological processes and spatial distribution in hadal zone

(A) The comparison of ecological processes of hadal zone and reported habitats (the reference number was consistent with that in the main text). The SRGs and ASVs were used in the MEER dataset. The ecological processes included homogeneous selection (HoS), heterogeneous selection (HeS), dispersal limitation (DL), drift (DR), and homogenizing dispersal (HD).

(B) The ecological processes of the Philippine Basin (PB), Yap Trench (YT), and Mariana Trench (MT), as well as the bottom (Bt), northern slope (NS), and southern slope (SS) within the MT based on SRG.

(C) Spatial distribution of ecological driving forces in the hadal zone based on SRG. The gray area in panel C represents the area for which a reliable interpolation could not be obtained due to a lack of sampling sites.

water depth, both across different hadal zones and within the MT (Figure 3C).

Vertical distribution of the microbial community with sediment depth and corresponding ecological driving forces

Sediment depth was considered to reflect chronological order in the depositional time and redox gradient.⁶⁴ Here, we conducted vertical analysis alongside sediment depth with pushcores of 30 cm (2 cm for each layer), which composed 94.8% of the sediment samples from the MT. Vertical profiling revealed systematic decreases in alpha diversity metrics, including Shannon index and phylogenetic diversity, with increasing sediment depth (Figure 4A). Similarly, the proportion of unreported SRGs showed a consistent decline along the depth gradient (Figure 4B).

The most abundant microbial taxa, archaeal phylum Thermoarchaeota and bacterial phylum Pseudomonadota, exhibited distinct vertical distribution patterns (Figure 4C). At the trench bottom, both phyla showed decreasing abundance with increasing sediment depth. By contrast, along northern and southern slopes, Thermoarchaeota abundance increased with sediment depth while Pseudomonadota remained relatively stable. These contrasting distribution patterns between trench bottom and slopes are consistent with previous observations in the MT.¹⁷

Concurrently, the contributions of HoS decreased with sediment depth, while DL showed an inverse trend (Figure 4D). In addition to HoS and DL, HeS also contributed to the microbial community assembly, especially at the bottom of the MT, with its contribution increasing from 3.6% at the surface (0–2 cm) to

for merely 1.4% of the microbial community assembly, while HoS (50.0%) and DL (45.9%) were predominant.

To elucidate the ecological mechanisms underlying variations in both taxonomic and functional community structures, we focused on SRG-based results. HoS (50.5%–55.2%) and DL (36.9%–43.9%) were the two main ecological forces driving microbial community assembly across the three hadal regions (PB, YT, and MT). Among them, MT presented the lowest proportion of HoS but the highest proportion of DL (Figure 3B). Within MT, the trench bottom displayed the lowest proportion of HoS (32.0%) but the highest proportion of DL (57.7%), contrasting with the northern slope (HoS: 57.7%, DL: 36.4%) and southern slope (HoS: 57.3%, DL: 38.9%) (Figure 3B). Generally, a decreasing trend of HoS but an increasing trend of DL and HeS were observed with increasing

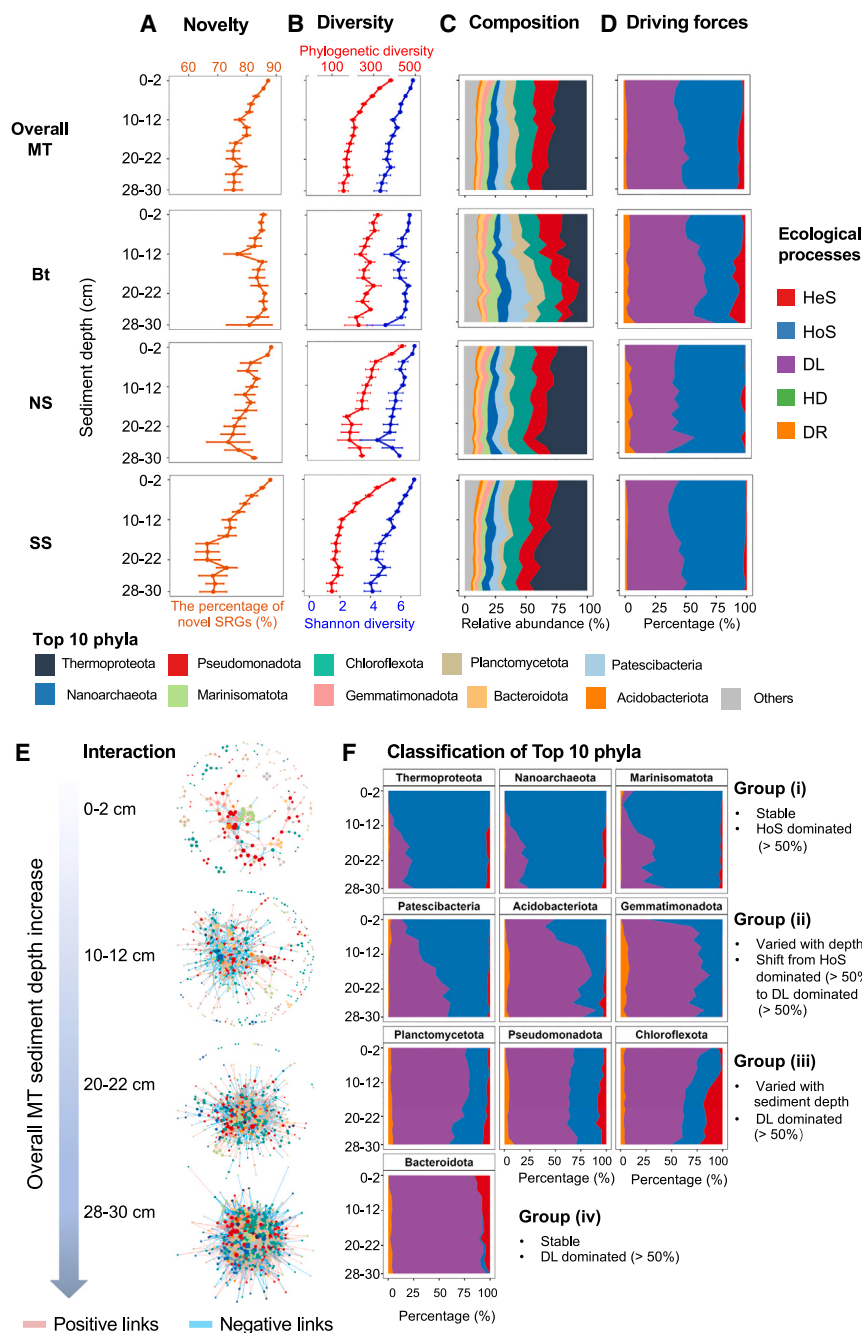


Figure 4. Vertical distribution of the microbial community with sediment depth and corresponding ecological driving forces

(A–D) (A) SRG-based microbial novelty (data are represented as mean \pm SD), (B) diversity (data are represented as mean \pm SD), (C) composition, and (D) driving forces in the Mariana Trench (MT), as well as the bottom (Bt), northern slope (NS), and southern slope (SS) within the MT along the sediment depth. The driving forces included heterogeneous selection (HeS), homogeneous selection (HoS), dispersal limitation (DL), homogenizing dispersal (HD), and drift (DR).

(E) SRG-based microbial networks in the MT. (F) The variations in the relative importance of the driving forces of the top 10 abundant phyla within the MT along the sediment depth gradient. See also Figures S3 and S4 and Table S3.

sediment layers. The average connection degree of 5.24–23.27 in the deeper layer (20–30 cm) was substantially greater than that in the surface layer (0–10 cm), with an average degree of 2.36–3.19. Similarly, we detected increases in the total number of nodes, links, and density with increasing sediment depth (Figure S3). These network indices revealed that network complexity increased with sediment depth, indicating more microbial interactions (both cooperation and competition) in deeper sediment layers.

Six SRG pairs exhibited consistent co-occurrence patterns across all 15 depth-specific networks, indicating stable cooperative relationships (Table S3). Analysis of unique KEGG orthologs (KOs) within each pair revealed complementary metabolic pathways. A representative example includes a pair of Pseudomonadota SRGs: the Kiloniellales member (FDZ074-GRW12-14.bin.32) possesses genes for aromatic compound degradation (e.g., catechol via *catA*, hydroxyquinol via *chqB*, and benzoyl-CoA via *boxB*), while its Rhodospirillales partner (FDZ077-WuWW16-18.bin.11) incorporates the resulting metabolites (e.g., succinyl-CoA via *sucC* and acetoacetyl-CoA via *atoB*) into the citrate cycle (TCA cycle). In porphyrin biosynthesis, the Kiloniellales SRG contains genes (*hemD*, *hemE*, *hemN*, and *hemH*) for *de novo* heme synthesis from hydroxymethylbilane, while the Rhodospirillales SRG produces its derivatives, including siroheme (*cobA* and *cysG*) and heme O (*COX10*). Furthermore, the Rhodospirillales SRG contains genes to synthesize trehalose (*otsA* and *otsB*) from Kiloniellales-produced UDP-glucose, potentially enhancing piezotolerance for both species. This metabolic complementarity suggests that microbial interactions through

13.8% in the deeper layer (26–28 cm). The vertical variation in ecological driving forces suggests that microenvironmental conditions change with sediment depth, influencing the relative abundance of dominant phyla. This observation aligns with previous hadal studies showing significant community changes along redox gradients.⁵³

We further constructed microbial taxonomic co-occurrence networks at each sediment layer to assess potential microbial interactions with sediment depth in the MT (Figures 4E and S3). More intense connections were generally observed in the deeper

sediment layers. The average connection degree of 5.24–23.27 in the deeper layer (20–30 cm) was substantially greater than that in the surface layer (0–10 cm), with an average degree of 2.36–3.19. Similarly, we detected increases in the total number of nodes, links, and density with increasing sediment depth (Figure S3). These network indices revealed that network complexity increased with sediment depth, indicating more microbial interactions (both cooperation and competition) in deeper sediment layers.

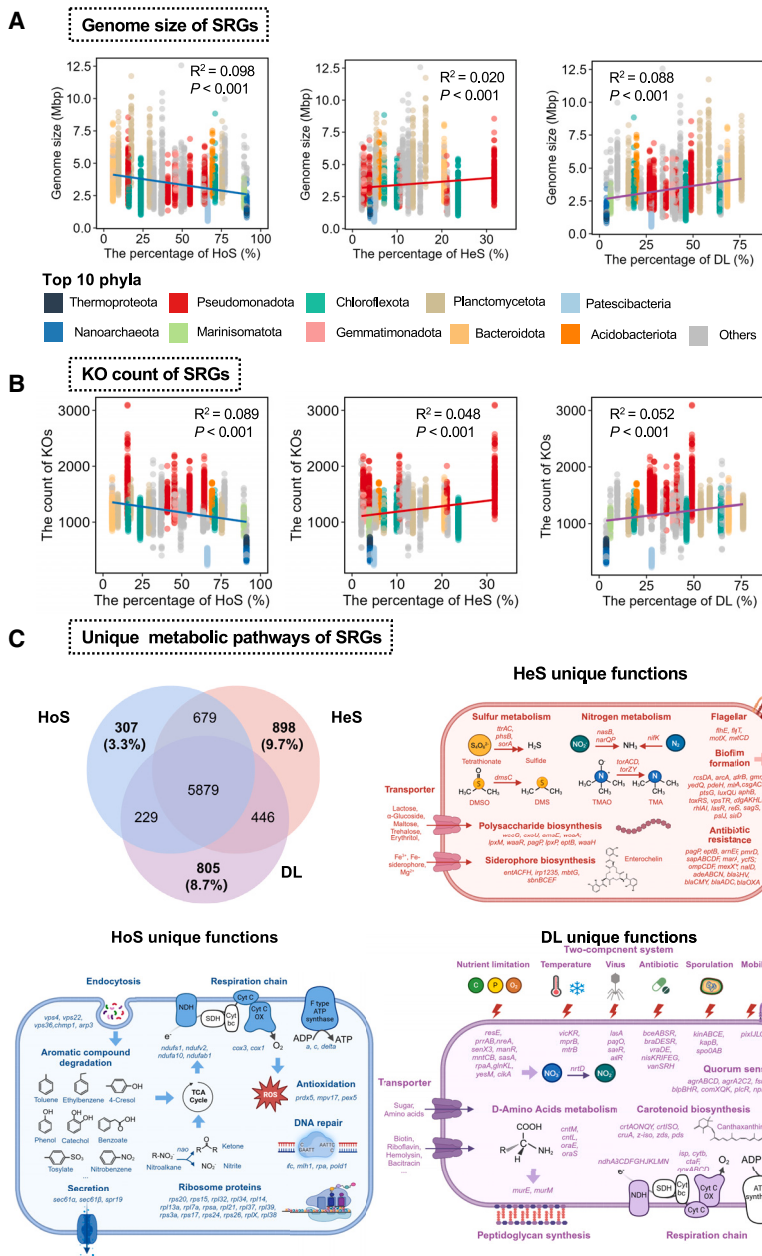


Figure 5. Ecological processes correlated with genomic traits and metabolic preference

The correlation of the percentage of main driving forces and genome size (A) as well as KO count (B) of SRGs. The main driving forces included homogeneous selection (HoS), heterogeneous selection (HeS), and dispersal limitation (DL) (C) Venn diagram of KO count of SRGs selected by main driving forces and the unique metabolic pathways. Pathways were drawn in BioRender.com. Gene abbreviations associated in each function were shown in italic style, which was followed the KO naming system. See also [Figure S5](#) and [Tables S4](#) and [S5](#).

a transition from HoS-dominated (>50.0%) to DL-dominated (>50.0%) processes along the sediment depth gradient. Group (3) included Planctomycetota, Pseudomonadota, and Chloroflexota, which were dominated by DL (>50.0%), but the proportion changed with sediment depth. Group (4), including Bacteroidota, presented high and stable relative importance (>50.0%) of DL.

Ecological processes correlated with genomic traits and metabolic preference

SRG-based analysis enabled the detection of genomic traits and metabolic potential in relation to ecological driving forces. Given the dominance of HoS and DL in the hadal zone, along with the sediment-depth-related HeS, we investigated how these driving forces contributed to taxonomic novelty, genomic traits, and metabolic potentials ([Figures 5A](#) and [S5](#)). We measured the RED value of good-quality SRGs (completeness > 75% and contamination < 10%) in conjunction with the relative importance of their ecological processes. Using the top 10

complementary functions become increasingly crucial for survival at greater sediment depths.

Finally, we observed distinct patterns of the ecological driving forces along sediment depth within the MT for various microbial taxa, especially the top 10 abundant phyla ([Figures 4F](#) and [S4](#)). These dominant phyla were further classified into four groups according to the shifting pattern of driving forces, which could help to acknowledge the taxon-specific community assembly strategies: group (1), including Thermoproteota, Nanoarchaeota, and Marinisomatota, exhibited high (>50.0%) relative importance of HoS, remaining stable across the sediment depth gradient. Group (2) comprised Patescibacteria, Acidobacteriota, and Gemmatimonadota, which showed

abundant phyla as examples, HoS, DL, and HeS collectively contributed to taxonomic novelty ([Figure S5](#)).

We further correlated genome size, G+C content, KO counts, predicted mean generation time, and optimal growth temperature of good-quality SRGs with their ecological driving forces ([STAR Methods](#), [Figure S5](#)). Notably, both genome size and KO counts showed significant negative correlations with HoS percentage (t test, $p < 0.001$) but positive correlations with DL and HeS percentages (t test, $p < 0.001$) ([Figures 5A](#) and [5B](#)), indicating HoS and DL/HeS shaped distinct adaptation strategies in hadal microbiome.

To investigate unique metabolic capabilities enriched by HoS, DL, and HeS, we classified SRGs according to relative

importance of these driving forces (Table S4) and identified their unique KOs (Table S5).

(1) HoS-dominated SRGs (HoS > 50.0%), primarily Thermoproteota, Nanoarchaeota, Marinisomatota, and Planctomycetota, of which 307 exclusive KOs exhibited enrichment in two major functions (Figure 5C; Table S5). The first category involved in aromatic compound degradation includes genes for toluene (e.g., *tmoA* and *tmoB*), ethylbenzene (e.g., *etbAa*), and nitrobenzene (e.g., *nahAb*) metabolism linked to the TCA cycle. The presence of these genes suggests aromatic compounds serve as available carbon sources in nutrient-limited hadal environments. Complementing this, endocytosis-associated genes (e.g., *vps4*, *vps22*, *vps36*, *chmp1*, and *arp3*) indicate potential mechanisms for direct uptake of refractory organic matter, including aromatic compounds, from the surrounding environment. The second major category encompasses antioxidation strategies against reactive oxygen species (ROS), featuring genes of peroxiredoxin 5 (*prdx5*), peroxin-5 (*pex5*), and Mpv17-like protein (*mpv17*). Besides the antioxidation, genes encoding DNA repair system (e.g., *mlh1*, *rpa*, and *pold1*), which are commonly used to protect against ROS damage of nucleotides, were also discovered. Together, these genes represent a universal adaptation mechanism to hadal conditions, as both high hydrostatic pressure⁶⁵ and near-freezing cold temperature⁶⁶ induce ROS formation, presenting a common challenge for hadal microorganisms.

(2) DL-dominated SRGs (DL > 50.0%), primarily comprising Planctomycetota, Bacteroidota, and Chloroflexota, exhibited 898 exclusive KOs enriched in environmental sensing systems (Figure 5C; Table S5). Unique KOs mainly involved in two-component systems responding to temperature (e.g., *vickR*, *mprB*, and *mtrB*), antibiotics (e.g., *bceABSR*, *braDESR*, *vraDE*, *nisKRIFEG*, and *vanSRH*), viruses (e.g., *lasA*, *pagO*, *saeR*, and *arlR*), sporulation signals (e.g., *kinABCE*, *kapB*, and *spo0AB*), and mobility cues (e.g., *pixJLGH*). Additionally, quorum sensing genes (e.g., *argABCD*, *fsrAC*, *blpBHR*, *comXQK*, and *nisRK*), transporters for various carbon sources (sugars and amino acids), and cofactors (biotin and riboflavin) were also observed. These patterns suggest that DL reflects limited microbial dispersal, with DL-dominated taxa specialized in responding to localized microenvironmental variations. Notably, two putative high-level undocumented lineages, MEER-01 and MEER-02, were also classified as DL-dominated. Beyond exhibiting the characteristic DL-associated functions mentioned above, both lineages possessed distinctive capabilities, such as special aromatic compound (naphthalene) degradation, highlighting DL's role in driving both functional versatility and taxonomic novelty in hadal environments.

(3) HeS-impacted SRGs (HoS < 50.0% and DL < 50.0%, HeS up to 31.7%), including Pseudomonadota and some Chloroflexota, of which 805 exclusive KOs exhibited enrichment in genes related to diverse anaerobic electron acceptors, such as nitrite reduction (e.g., *nasB* and *narQP*), tetrathionate reduction (e.g., *ttrAC*, *phsB*, and *sorA*), and iron transporter (e.g., *fecB*, *fecC*, *fecD*, *fecE*, and *fecB*). Additionally, a series of genes related to biofilm formation (e.g., *rcsDA*, *arcA*, *adrB*, *gmr*, and *yedQ*), antibiotic resistance (e.g., *pagP*, *eptB*, *arnEF*, *pmrAB*, and *sapABCD*), and flagellar assembly (e.g., *flhE*, *flgT*, *motX*, and *motCD*) were detected (Figure 5C; Table S5). The

HeS-enriched functions indicated adaptations to changing redox gradients and increased microbial interactions with sediment depth. These findings provide essential ecological evidence supporting the established relationship between redox gradients and vertical microbial community succession in hadal sediments.⁵³

To validate our findings, we performed parallel ASV-based analyses, which largely confirmed the SRG-based results, particularly in identifying dominant ecological processes across major taxonomic groups. However, three groups—Thermoproteota, Nanoarchaeota, and Marinisomatota—showed contrasting patterns, appearing DL-dominated in ASV-based analysis but HoS-dominated in SRG-based analysis. This discrepancy could be illustrated by Thermoproteota: while 16S rRNA analysis detected 4,495 AOA and 1,004 Bathyarchaeia ASVs, only 33 high-quality AOA SRGs were available for ecological analysis. The DL-dominance in ASV analysis reflects stochastic cross-sample diversity from 16S rRNA marker gene variants. However, given known limitations of ASV-based approaches—including 16S rRNA gene copy number variations and bias of polymerase chain reaction (PCR) efficiency against AOA^{67,68}—we consider the SRG-based results more reliable. The SRG approach directly links taxonomic information to adaptive traits, making the HoS-dominated classification more convincing from a functional perspective. Similar reasoning applies to Nanoarchaeota and Marinisomatota, where genome-level evidence better reflects environmental selection's role in community assembly.

DISCUSSION

This study presents a comprehensive investigation of hadal microbial communities, spanning three geographically proximate yet distinct hadal zones. Our sampling strategy primarily targeted unexplored areas, achieving extraordinary coverage of diverse MT topography, including the Challenger Deep's eastern and western depressions, trench axis, and both slopes. We extended sampling to previously unexplored region at the deepest region in YT (~9,000 m) and included PB samples as a comparative hadal environment. This systematic approach generated the MEER dataset, revealing extraordinary taxonomic novelty, with 89.4% of species previously undocumented. Comparative analyses with the global ocean microbiome (OMD),³⁰ deep-sea sediments (typically < 4,000 m depth),^{31–47} and previously reported hadal samples^{5,9,10,12,13,48} demonstrate the microbial assemblages inhabiting hadal extreme environments. The exceptional taxonomic novelty underscores the value of our extensive sampling effort in uncovering the distinct microbial diversity of Earth's deepest oceans.

Our study focuses on a long-standing goal in microbial ecology: elucidating how environments shape microbial communities, especially in extreme conditions. Unlike other environments such as shallower marine sediments,⁶³ soil,^{23,57–59} or water,^{22,60–62} where DR played an unignorable role driving community assembly, hadal microbiomes are primarily shaped by HoS and DL. This simplified pattern of ecological processes in the hadal zone provides an ideal system to investigate environment-microbe relationships. The minimal role of DR in the hadal zone suggested that the strong selective pressures exerted by

this extreme environment. The dominance of HoS in shaping hadal microbiomes reflects the pervasive influence of extreme hadal conditions, characterized by functional adaptations to high pressure and cold (antioxidation to counter ROS induced by both high pressure⁶⁵ and low temperature⁶⁶) and oligotrophy (aromatic compound utilization addressing limited nutrient availability⁶⁹). Notably, HoS accounts for over 90% of the ecological processes on AOA SRGs within Thermoproteota, suggesting that universal environmental stresses selectively drive the phylo-type differentiation of this crucial functional group in hadal ecosystems.

Complementing these broad environmental pressures, DL and HeS suggested the influence of additional environmental factors on hadal microorganisms. DL highlights the role of microbial interactions,⁷⁰ while HeS points to the importance of redox gradients⁵³ along sediment depth in shaping microbial communities. Previous studies demonstrated that Chloroflexi in hadal sediments exhibit heterotrophic lifestyles responsive to varying nutrient conditions,⁵ while anammox bacteria Brocadiales occupy specific niches along sedimentary redox gradients at the oxic-nitrogenous transition zone.¹⁹ Here we found both Chloroflexota and Brocadiales were classified as DL-dominated with substantial HeS contribution, providing ecological insights to elucidate the previous observations. In addition, the increased significance of DL at the MT bottom and the heightened importance of both DL and HeS in deeper sediment layers indicated that beyond high pressure and oligotrophy, additional factors shape hadal microbial communities. These include localized environmental stimuli (e.g., redox gradients, inter-species, and host-virus interactions) and factors influencing microbial community interchange (such as fluid and sediment dynamics), which collectively contribute to the exceptional taxonomic novelty and diversity. Further exploration of how ocean currents⁷¹ and seafloor topography⁷² affect localized environmental conditions in hadal zone will be addressed in upcoming MEER series publications.

According to the correlations between distinct ecological processes and genomic/metabolic traits, we could identify two distinct adaptation strategies: streamlined and versatile. The streamlined strategy, reflected in HoS-dominant microorganisms, is characterized by smaller genomes and focused metabolic potentials. This strategy was aligned with previous cultivation experiments comparing shallow marine *Colwellia* strains (~5.4 Mbps genome) with their piezophilic relatives (~4.3 Mbps) from the MT bottom.⁷³ The consistency between our data-driven results and culturable studies suggests genome streamlining as a potential hallmark of hadal piezophiles, potentially expanding their known diversity beyond the ~70 isolates reported over four decades.⁷⁴ Conversely, DL-dominated and HeS-impacted microorganisms represent a versatility strategy, featuring larger genome size and diverse metabolic capabilities indicative of an opportunistic (R-strategy) lifestyle. This strategy resembles the “bathotypes” observed in shallower deep-sea microorganisms,⁷⁵ suggesting it may not represent long-term hadal adaptation. These contrasting ecological strategies not only explain the distinct evolutionary trajectories reported between the HoS-dominated AOA and the DL-dominated Chloroflexota and anammox bacteria^{5,18,19} but also provide a framework for comprehensively inves-

tigating adaptation mechanisms across diverse taxa in hadal environments. Further evidence of microbial activity for these adaptation strategies will be explored in future metaproteomic and culturomic experiments within the MEER series.

Finally, compared with canonical 16S rRNA gene ASV-based ecological analysis, shotgun metagenome SRG-based approaches established in this study successfully connected ecological processes, metabolic potentials, genome traits, and extreme environments. The SRG-based approach proves particularly valuable in studying less-explored environments like the hadal zone, where many species remain unknown. Through rigorous assembly and quality control procedures, each SRG represents a microbial species present in the samples, with its genomic content enabling direct and comprehensive assessment of metabolic potential and adaptation mechanisms.^{76,77} By contrast, ASV generation can be affected by multiple factors, including 16S rRNA gene copy numbers, PCR amplification biases, and artifacts during sequencing and bioinformatic analyses, such as consistently underestimation of Thermoproteota abundances⁶⁷ but overestimation of Bacteroidota abundance.⁷⁸ These differential patterns align with our observations between SRG-based and ASV-based results. Nevertheless, despite methodological variations affecting such taxonomic groups, the majority of taxa exhibited comparable abundance patterns between both analytical approaches. Consequently, unclassified ASVs cannot confidentially indicate the presence of unreported species, nor can they provide insights into metabolic capabilities or adaptation strategies of the undescribed organisms. Although the ASV approach maintains value for its broader taxonomic coverage and higher data acquisition success rate (1,587 vs. 1,194 from 1,648 total samples), these inherent methodological differences explain the observed variations in diversities and ecological factors between ASV-based and SRG-based results. Despite these methodological discrepancies, the overall trends and conclusions drawn from both approaches remain largely consistent, reinforcing the robustness of our main findings. Therefore, the SRG-based strategy proposed in this study offers significant value in microbial studies and demonstrates wide applicability, particularly in the exploration of extreme and understudied ecosystems.

Limitations of the study

Despite our extensive sampling effort of 1,648 sediment samples, the vast expanse and heterogeneity of hadal environments mean our findings may not fully represent all global hadal microbial communities. While our metagenomic approach provides powerful insights into genetic potential, it cannot directly inform on the actual physiological state of microorganisms or the functions actively being expressed. Future integration of metaproteomics and culturomics will be crucial to bridge this gap. Additionally, our study does not capture temporal dynamics or seasonal variations that may influence hadal ecosystems, highlighting the need for long-term monitoring. Furthermore, this study focuses primarily on prokaryotic communities, leaving the complex interactions between prokaryotes, eukaryotes (especially hadal fauna), and viruses unexplored. A more holistic ecosystem-level investigation and discussion are necessary in future research.

The extreme nature of hadal environments poses significant challenges for acquiring comprehensive environmental data. This scarcity of environmental parameters, compared with the wealth of microbiome data, hampers our ability to fully decipher the complex interplay between microbial communities and their unique habitats. Given the technical constraints of *in situ* measurements, microbial-based approaches that infer environmental characteristics from microbiome information serve not only as an alternative strategy but also as a promising framework for gaining insights into hadal geography, geochemical processes, and other non-biological fields. The inability to replicate hadal conditions in laboratory settings further constrains our capacity for experimental validation of the proposed ecological theories and metabolic predictions. Continued improvement in sampling techniques, preservation methods, and environmental data collection will be crucial for capturing an even more accurate and comprehensive picture of hadal microbial communities and their ecological dynamics. These challenges set the stage for future investigations, including forthcoming articles in the MEER series, which aim to provide preliminary explorations of these broader aspects and push the boundaries of our understanding of life in Earth's most extreme environments.

RESOURCE AVAILABILITY

Lead contact

Further information and requests for resources and reagents should be directed to and will be fulfilled by the lead contact, Xiang Xiao (zxiao2018@sjtu.edu.cn).

Materials availability

This study did not generate new unique reagents.

Data and code availability

All data can be viewed in NODE (<http://www.biosino.org/node>) by pasting the accession OEP004067 into the text search box or through the URL: <https://www.biosino.org/node/project/detail/OEP004067> and has been deposited at CNSA with the accession CNP0004890 (<https://db.cngb.org/search/project/CNP0004890/>). The SRGs have been deposited in eMSG (<https://www.biosino.org/elmsg/index>) under accession numbers LMSG_G000 037053.1 – LMSG_G000044616.1. The code for quality control, assembly, binning, classification, and abundance profiling is accessible at https://github.com/meer-trench/genome_catalogue. Additionally, the code for downstream ecological analyses can be found at <https://doi.org/10.5281/zenodo.13317475>. These data and codes are publicly available as of the date of publication. Any additional information required to reanalyze the data reported in this work is available from the [lead contact](#) upon request.

Published databases and datasets used as references in this study, including OMD (<https://microbiomics.io/ocean/>), GTDB database (<https://gtdb.ecogenomic.org/>), SILVA database (<https://www.arb-silva.de/>), and Greengenes2 database (https://ftp.microbio.me/greengenes_release/2022.10/) can be accessed through their own URLs respectively.

ACKNOWLEDGMENTS

We would like to thank the pilots of the full-ocean-depth HOV *Fendouzhe* and the crew of the R/V "Tan Suo Yi Hao" for their professional service during the cruise of TS21 in 2021, as well as the cruise support from Hainan Deep-Sea Technology Innovation Center. This work was financially supported by the National Natural Science Foundation of China (grant nos. 41921006, 92451301, 42106087, and 92251303), the National Key R&D Program of China (grant nos. 2022YFC2805404, 2022YFC2805304, and 2017YFC0306502), the Major Science and Technology Research Project of Sanya Yazhou Bay Science and

Technology City (grant SKJC-2021-01-001), and the Strategic Priority Research Program of the Chinese Academy of Sciences (grant no. XDA22040600). We extend our gratitude to NODE (<https://www.biosino.org/node/>) maintained by the Bio-Med Big Data Center, SINH, CAS, for providing well-curated, high-quality public metagenomic data for deep-sea sediments. This study was also supported by the High-performance Computing Platform of Yazhou Bay Science and Technology City Advanced Computing Center (YZBSCACC). We also thank Dr. Daliang Ning from the University of Oklahoma for his constructive comments and help with ICAMP analysis.

AUTHOR CONTRIBUTIONS

Conceptualization, Jian Wang, K.D., X. Xiao, X. Xu, S.L., W.-J.Z., M.H., and W.Z.; methodology, Z.S., J.L., Q.Q., W.Z., Y.W., Q.J., C.T., Jing Wang, A.H., and S.H.; software, Z.S., J.L., Q.Q., J. Zhu, C.F., Y.W., Jing Wang, A.H., S.H., and W.Z.; validation, X. Xu, S.L., and X. Xiao; formal analysis, Z.S., Q.Q., J. Zhu, Jianwei Chen, J.L., C.F., Jing Wang, A.H., S.H., W.Z., J.F., C.Z., Jun Wang, and X.W.; investigation, Jian Wang, K.D., X. Xiao, X. Xu, S.L., W.-J.Z., W.Z., Q.J., X.L., G.M., C.C., S. Cai, S. Chen, D.L., S.L., T.S., L.T., H.Z., Y.Z., and L.L.; resources, K.D., Jian Wang, X. Xu, X. Xiao, S.L., J.L., C.C., W.-J.Z., B.W., L.C., H.Y., Jiayu Chen, X.W., G.H., F.J., Q.C., H.C., M.N., and F.M.; data curation, Z.S., C.F., Y.W., L.Z., S.X., T.Y., and W.W.; writing – original draft, M.H., W.Z., J. Zhu, Q.Q., Z.S., C.F., Jianwei Chen, and H.C.; writing – review & editing, X. Xiao, W.Z., S.H., Jing Wang, M.H., Z.S., J. Zhu, B.W., Jianwei Chen, C.F., K.K., X.W., Y.Y., and J. Zhou.; visualization, W.Z., Z.S., Q.Q., J. Zhu, S.H., Jing Wang, Jianwei Chen, C.F., Jun Wang, and A.H.; supervision, X. Xiao, S.L., X. Xu, W.Z., W.-J.Z., and J.L.; project administration, X. Xu, X. Xiao, S.L., W.-J.Z., B.W., Y.G., M.H., W.Z., and H.C.; funding acquisition, K.D., Jian Wang, and X. Xiao.

DECLARATION OF INTERESTS

The authors declare no competing interests.

STAR★METHODS

Detailed methods are provided in the online version of this paper and include the following:

- KEY RESOURCES TABLE
- EXPERIMENTAL MODEL AND STUDY PARTICIPANT DETAILS
- METHOD DETAILS
 - Sample collection and DNA extraction
 - 16S rRNA gene amplicon sequencing and analysis
 - Metagenomic sequencing, binning and annotation
 - Biogeographic distribution analysis
 - Microbial community assembly calculation
 - Molecular ecological network construction and analyses
 - Genomic and physiological trait prediction of SRGs

SUPPLEMENTAL INFORMATION

Supplemental information can be found online at <https://doi.org/10.1016/j.cell.2024.12.036>.

Received: October 19, 2023

Revised: August 18, 2024

Accepted: December 25, 2024

Published: March 6, 2025

REFERENCES

1. Stewart, H.A., and Jamieson, A.J. (2018). Habitat heterogeneity of hadal trenches: Considerations and implications for future studies. *Prog. Oceanogr.* 161, 47–65. <https://doi.org/10.1016/j.pcean.2018.01.007>.

2. Stewart, H.A., and Jamieson, A.J. (2019). The five deeps: The location and depth of the deepest place in each of the world's oceans. *Earth Sci. Rev.* 197, 102896. <https://doi.org/10.1016/j.earscirev.2019.102896>.
3. Jamieson, A. (2015). *The Hadal Zone: Life in the Deepest Oceans* (Cambridge University Press).
4. Jamieson, A.J., Fujii, T., Mayor, D.J., Solan, M., and Priede, I.G. (2010). Hadal trenches: the ecology of the deepest places on Earth. *Trends Ecol. Evol.* 25, 190–197. <https://doi.org/10.1016/j.tree.2009.09.009>.
5. Liu, R., Wei, X., Song, W., Wang, L., Cao, J., Wu, J., Thomas, T., Jin, T., Wang, Z., and Wei, W. (2022). Novel Chloroflexi genomes from the deepest ocean reveal metabolic strategies for the adaptation to deep-sea habitats. *Microbiome* 10, 75. <https://doi.org/10.21203/rs.3.rs-254541/v1>.
6. He, L., Huang, X., Zhang, G., Yuan, L., Shen, E., Zhang, L., Zhang, X.-H., Zhang, T., Tao, L., and Ju, F. (2022). Distinctive signatures of pathogenic and antibiotic resistant potentials in the hadal microbiome. *Environ. Microbiome* 17, 19. <https://doi.org/10.1186/s40793-022-00413-5>.
7. Zhao, J., Jing, H., Wang, Z., Wang, L., Jian, H., Zhang, R., Xiao, X., Chen, F., Jiao, N., and Zhang, Y. (2022). Novel viral communities potentially assisting in carbon, nitrogen, and sulfur metabolism in the upper slope sediments of Mariana Trench. *mSystems* 7, e0135821. <https://doi.org/10.1128/msystems.01358-21>.
8. Zhang, X., Wu, K., Han, Z., Chen, Z., Liu, Z., Sun, Z., Shao, L., Zhao, Z., and Zhou, L. (2022). Microbial diversity and biogeochemical cycling potential in deep-sea sediments associated with seamount, trench, and cold seep ecosystems. *Front. Microbiol.* 13, 1029564. <https://doi.org/10.3389/fmicb.2022.1029564>.
9. Liu, Y., Zhang, Z., Ji, M., Hu, A., Wang, J., Jing, H., Liu, K., Xiao, X., and Zhao, W. (2022). Comparison of prokaryotes between Mount Everest and the Mariana Trench. *Microbiome* 10, 215. <https://doi.org/10.1186/s40168-022-01403-y>.
10. Zhou, Y.L., Mara, P., Cui, G.J., Edgcomb, V.P., and Wang, Y. (2022). Microbiomes in the Challenger Deep slope and bottom-axis sediments. *Nat. Commun.* 13, 1515. <https://doi.org/10.1038/s41467-022-29144-4>.
11. Liu, J., Li, D.-W., He, X., Liu, R., Cheng, H., Su, C., Chen, M., Wang, Y., Zhao, Z., Xu, H., et al. (2024). A unique seafloor microbiosphere in the Mariana Trench driven by episodic sedimentation. *Mar. Life Sci. Technol.* 6, 168–181. <https://doi.org/10.1007/s42995-023-00212-y>.
12. Chen, P., Zhou, H., Huang, Y., Xie, Z., Zhang, M., Wei, Y., Li, J., Ma, Y., Luo, M., Ding, W., et al. (2021). Revealing the full biosphere structure and versatile metabolic functions in the deepest ocean sediment of the Challenger Deep. *Genome Biol.* 22, 207. <https://doi.org/10.1186/s13059-021-02408-w>.
13. Wang, H., Wang, M., Fan, S., Lu, J., Lan, Y., Li, M., Li, J., Liu, R., Sun, J., Fang, J., et al. (2021). Culture enrichment combined with long-read sequencing facilitates genomic understanding of hadal sediment microbes. *Front. Mar. Sci.* 8, 754332. <https://doi.org/10.3389/fmars.2021.754332>.
14. Tarn, J., Peoples, L.M., Hardy, K., Cameron, J., and Bartlett, D.H. (2016). Identification of free-living and particle-associated microbial communities present in hadal regions of the Mariana Trench. *Front. Microbiol.* 7, 665. <https://doi.org/10.3389/fmicb.2016.00665>.
15. Liu, R., Wang, L., Wei, Y., and Fang, J. (2018). The hadal biosphere: Recent insights and new directions. *Deep Sea Res. II* 155, 11–18. <https://doi.org/10.1016/j.dsr2.2017.04.015>.
16. Huang, J.M., and Wang, Y. (2020). Genomic differences within the phylum Marinimicrobia: from waters to sediments in the Mariana Trench. *Mar. Genomics* 50, 100699. <https://doi.org/10.1016/j.margen.2019.100699>.
17. Hiraoka, S., Hirai, M., Matsui, Y., Makabe, A., Minegishi, H., Tsuda, M., Juliarni, R., Rastelli, E., Danovaro, R., Corinaldesi, C., et al. (2020). Microbial community and geochemical analyses of trans-trench sediments for understanding the roles of hadal environments. *ISME J.* 14, 740–756. <https://doi.org/10.1038/s41396-019-0564-z>.
18. Zhong, H., Lehtovirta-Morley, L., Liu, J., Zheng, Y., Lin, H., Song, D., Todd, J.D., Tian, J., and Zhang, X.-H. (2020). Novel insights into the Thaumarchaeota in the deepest oceans: their metabolism and potential adaptation mechanisms. *Microbiome* 8, 78. <https://doi.org/10.1186/s40168-020-00849-2>.
19. Thamdrup, B., Schauberger, C., Larsen, M., Trouche, B., Maignien, L., Arnaud-Haond, S., Wenzhöfer, F., and Glud, R.N. (2021). Anammox bacteria drive fixed nitrogen loss in hadal trench sediments. *Proc. Natl. Acad. Sci. USA* 118, e2104529118. <https://doi.org/10.1186/s40168-022-01263-6>.
20. Li, C., Wang, L., Ji, S., Chang, M., Wang, L., Gan, Y., and Liu, J. (2021). The ecology of the plastisphere: Microbial composition, function, assembly, and network in the freshwater and seawater ecosystems. *Water Res.* 202, 117428. <https://doi.org/10.1016/j.watres.2021.117428>.
21. Sun, C., Zhang, B., Ning, D., Zhang, Y., Dai, T., Wu, L., Li, T., Liu, W., Zhou, J., and Wen, X. (2021). Seasonal dynamics of the microbial community in two full-scale wastewater treatment plants: diversity, composition, phylogenetic group based assembly and co-occurrence pattern. *Water Res.* 200, 117295. <https://doi.org/10.1016/j.watres.2021.117295>.
22. Ning, D., Wang, Y., Fan, Y., Wang, J., Van Nostrand, J.D., Wu, L., Zhang, P., Curtis, D.J., Tian, R., Lui, L., et al. (2024). Environmental stress mediates groundwater microbial community assembly. *Nat. Microbiol.* 9, 490–501. <https://doi.org/10.1038/s41564-023-01573-x>.
23. Ning, D., Yuan, M., Wu, L., Zhang, Y., Guo, X., Zhou, X., Yang, Y., Arkin, A.P., Firestone, M.K., and Zhou, J. (2020). A quantitative framework reveals ecological drivers of grassland microbial community assembly in response to warming. *Nat. Commun.* 11, 4717. <https://doi.org/10.1038/s41467-020-18560-z>.
24. Dini-Andreote, F., Stegen, J.C., van Elsas, J.D., and Salles, J.F. (2015). Disentangling mechanisms that mediate the balance between stochastic and deterministic processes in microbial succession. *Proc. Natl. Acad. Sci. USA* 112, E1326–E1332. <https://doi.org/10.1073/pnas.1414261112>.
25. Gilbert, B., and Levine, J.M. (2017). Ecological drift and the distribution of species diversity. *Proc. Biol. Sci.* 284, 20170507. <https://doi.org/10.1098/rspb.2017.0507>.
26. Saccheri, I., and Hanski, I. (2006). Natural selection and population dynamics. *Trends Ecol. Evol.* 21, 341–347. <https://doi.org/10.1016/j.tree.2006.03.018>.
27. Yuan, M.M., Guo, X., Wu, L., Zhang, Y., Xiao, N., Ning, D., Shi, Z., Zhou, X., Wu, L., Yang, Y., et al. (2021). Climate warming enhances microbial network complexity and stability. *Nat. Clim. Chang.* 11, 343–348. <https://doi.org/10.1038/s41558-021-00989-9>.
28. Bartoš, O., Chmel, M., and Swierczková, I. (2024). The overlooked evolutionary dynamics of 16S rRNA revises its role as the “gold standard” for bacterial species identification. *Sci. Rep.* 14, 9067. <https://doi.org/10.1038/s41598-024-59667-3>.
29. Bowers, R.M., Kyrpides, N.C., Stepanauskas, R., Harmon-Smith, M., Doud, D., Reddy, T.B.K., Schulz, F., Jarett, J., Rivers, A.R., Eloe-Fadrosh, E.A., et al. (2017). Minimum information about a single amplified genome (MISAG) and a metagenome-assembled genome (MIMAG) of bacteria and archaea. *Nat. Biotechnol.* 35, 725–731. <https://doi.org/10.1038/nbt.3893>.
30. Paoli, L., Ruscheweyh, H.-J., Fomeris, C.C., Hubrich, F., Kautsar, S., Bhushan, A., Lotti, A., Clayssen, Q., Salazar, G., Milanese, A., et al. (2022). Biosynthetic potential of the global ocean microbiome. *Nature* 607, 111–118. <https://doi.org/10.1038/s41586-022-04862-3>.
31. Laso-Pérez, R., Hahn, C., van Vliet, D.M., Tegetmeyer, H.E., Schubotz, F., Smit, N.T., Pape, T., Sahling, H., Bohrmann, G., and Boetius, A. (2019). Anaerobic degradation of non-methane alkanes by “*Candidatus Methanoliparia*” in hydrocarbon seeps of the Gulf of Mexico. *mBio* 10, e01814-19. <https://doi.org/10.1128/mbio.01814-19>.

32. Zheng, X., Dai, X., Zhu, Y., Yang, J., Jiang, H., Dong, H., and Huang, L. (2022). (Meta)Genomic analysis reveals diverse energy conservation strategies employed by globally distributed Gemmatimonadota. *mSystems* 7, e0022822. <https://doi.org/10.1128/mSystems.00228-22>.
33. Jing, H., Wang, R., Jiang, Q., Zhang, Y., and Peng, X. (2020). Anaerobic methane oxidation coupled to denitrification is an important potential methane sink in deep-sea cold seeps. *Sci. Total Environ.* 748, 142459. <https://doi.org/10.1016/j.scitotenv.2020.142459>.
34. Lu, Y., Zhang, Y., Wang, J., Zhang, M., Wu, Y., Xiao, X., and Xu, J. (2022). Dynamics in bacterial community affected by mesoscale eddies in the northern slope of the South China Sea. *Microb. Ecol.* 83, 823–836. <https://doi.org/10.1007/s00248-021-01816-6>.
35. Heyerhoff, B., Engelen, B., and Bunse, C. (2022). Auxiliary metabolic gene functions in pelagic and benthic viruses of the Baltic Sea. *Front. Microbiol.* 13, 863620. <https://doi.org/10.3389/fmicb.2022.863620>.
36. Pelikan, C., Wasmund, K., Glombitza, C., Hausmann, B., Herbold, C.W., Flieder, M., and Loy, A. (2021). Anaerobic bacterial degradation of protein and lipid macromolecules in subarctic marine sediment. *ISME J.* 15, 833–847. <https://doi.org/10.1038/s41396-020-00817-6>.
37. Speth, D.R., Yu, F.B., Connon, S.A., Lim, S., Magyar, J.S., Peña-Salinas, M.E., Quake, S.R., and Orphan, V.J. (2022). Microbial communities of Auka hydrothermal sediments shed light on vent biogeography and the evolutionary history of thermophily. *ISME J.* 16, 1750–1764. <https://doi.org/10.1038/s41396-022-01222-x>.
38. Bell, E., Rattray, J.E., Sloan, K., Sherry, A., Pilloni, G., and Hubert, C.R.J. (2022). Hyperthermophilic endospores germinate and metabolize organic carbon in sediments heated to 80 °C. *Environ. Microbiol.* 24, 5534–5545. <https://doi.org/10.1111/1462-2920.16167>.
39. Zhang, T., Li, J., Wang, N., Wang, H., and Yu, L. (2022). Metagenomic analysis reveals microbiome and resistome in the seawater and sediments of Kongsfjorden (Svalbard, High Arctic). *Sci. Total Environ.* 809, 151937.
40. Baker, B. (2013). Insights into metabolisms of the cosmopolitan, enigmatic Miscellaneous Crenarchaeotal Group (MCG) in marine sediments. 10.25585/1487961.
41. Dombrowski, N., Teske, A.P., and Baker, B.J. (2018). Expansive microbial metabolic versatility and biodiversity in dynamic Guaymas Basin hydrothermal sediments. *Nat. Commun.* 9, 4999. <https://doi.org/10.1038/s41467-018-07418-0>.
42. Liu, J., Zhang, Y., Liu, J., Zhong, H., Williams, B.T., Zheng, Y., Curson, A.R.J., Sun, C., Sun, H., Song, D., et al. (2021). Bacterial dimethylsulfoniopropionate biosynthesis in the East China Sea. *Microorganisms* 9, 657. <https://doi.org/10.3390/microorganisms9030657>.
43. Song, D., Zhang, Y., Liu, J., Zhong, H., Zheng, Y., Zhou, S., Yu, M., Todd, J.D., and Zhang, X.H. (2020). Metagenomic insights into the cycling of dimethylsulfoniopropionate and related molecules in the eastern China marginal seas. *Front. Microbiol.* 11, 157. <https://doi.org/10.3389/fmicb.2020.00157>.
44. Bäckström, D., Yutin, N., Jørgensen, S.L., Dharamshi, J., Homa, F., Zarembo-Niedwiedzka, K., Spang, A., Wolf, Y.I., Koonin, E.V., and Ettema, T.J.G. (2019). Virus genomes from deep sea sediments expand the ocean megavirome and support independent origins of viral gigantism. *mBio* 10, e02497-18. <https://doi.org/10.1128/mbio.02497-18>.
45. Broman, E., Bonaglia, S., Holovachov, O., Marzocchi, U., Hall, P.O.J., and Nascimento, F.J.A. (2020). Uncovering diversity and metabolic spectrum of animals in dead zone sediments. *Commun. Biol.* 3, 106. <https://doi.org/10.1038/s42003-020-0822-7>.
46. Zhao, R., Summers, Z.M., Christman, G.D., Yoshimura, K.M., and Biddle, J.F. (2020). Metagenomic views of microbial dynamics influenced by hydrocarbon seepage in sediments of the Gulf of Mexico. *Sci. Rep.* 10, 5772. <https://doi.org/10.1038/s41598-020-62840-z>.
47. Leon Zayas, R., Bartlett, D., and Biddle, J. (2016). Microbial community composition and function in the Tonga Trench: from 400m below the sea surface to 9100m water depth and from 0 to 2 m below the seafloor. *Environ. Microbiol.*
48. Liu, J., Zheng, Y., Lin, H., Wang, X., Li, M., Liu, Y., Yu, M., Zhao, M., Pendentchouk, N., and Lea-Smith, D.J. (2019). Proliferation of hydrocarbon-degrading microbes at the bottom of the Mariana Trench. *Microbiome* 7, 1–13. <https://doi.org/10.1186/s40168-019-0652-3>.
49. Parks, D.H., Chuvochina, M., Rinke, C., Mussig, A.J., Chaumeil, P.-A., and Hugenholtz, P. (2022). GTDB: an ongoing census of bacterial and archaeal diversity through a phylogenetically consistent, rank normalized and complete genome-based taxonomy. *Nucleic Acids Res.* 50, D785–D794. <https://doi.org/10.1093/nar/gkab776>.
50. Parks, D.H., Chuvochina, M., Waite, D.W., Rinke, C., Skarshewski, A., Chaumeil, P.-A., and Hugenholtz, P. (2018). A standardized bacterial taxonomy based on genome phylogeny substantially revises the tree of life. *Nat. Biotechnol.* 36, 996–1004. <https://doi.org/10.1038/nbt.4229>.
51. Quast, C., Pruesse, E., Yilmaz, P., Gerken, J., Schweer, T., Yarza, P., Peplies, J., and Glöckner, F.O. (2013). The SILVA ribosomal RNA gene database project: improved data processing and web-based tools. *Nucleic Acids Res.* 41, D590–D596. <https://doi.org/10.1093/nar/gks1219>.
52. McDonald, D., Jiang, Y., Balaban, M., Cantrell, K., Zhu, Q., Gonzalez, A., Morton, J.T., Nicolaou, G., Parks, D.H., Karst, S.M., et al. (2024). GreenGenes2 unifies microbial data in a single reference tree. *Nat. Biotechnol.* 42, 715–718. <https://doi.org/10.1038/s41587-023-01845-1>.
53. Schauburger, C., Glud, R.N., Hausmann, B., Trouche, B., Maignien, L., Poulain, J., Wincker, P., Arnaud-Haond, S., Wenzhöfer, F., and Thamdrup, B. (2021). Microbial community structure in hadal sediments: high similarity along trench axes and strong changes along redox gradients. *ISME J.* 15, 3455–3467. <https://doi.org/10.1038/s41396-021-01021-w>.
54. Song, T., Liang, Q., Du, Z., Wang, X., Chen, G., Du, Z., and Mu, D. (2022). Salinity gradient controls microbial community structure and assembly in coastal solar salterns. *Genes* 13, 385. <https://doi.org/10.3390/genes13020385>.
55. Liu, X., Li, H., Song, W., and Tu, Q. (2023). Distinct ecological mechanisms drive the spatial scaling of abundant and rare microbial taxa in a coastal sediment. *J. Biogeogr.* 50, 909–919. <https://doi.org/10.1111/jbi.14584>.
56. Liu, L., Wang, N., Liu, M., Guo, Z., and Shi, S. (2023). Assembly processes underlying bacterial community differentiation among geographically close mangrove forests. *mLife* 2, 73–88. <https://doi.org/10.1002/mlf2.12060>.
57. Chen, D., Hou, H., Zhou, S., Zhang, S., Liu, D., Pang, Z., Hu, J., Xue, K., Du, J., Cui, X., et al. (2022). Soil diazotrophic abundance, diversity, and community assembly mechanisms significantly differ between glacier riparian wetlands and their adjacent alpine meadows. *Front. Microbiol.* 13, 1063027. <https://doi.org/10.3389/fmicb.2022.1063027>.
58. He, Y., Tripathi, B.M., Fang, J., Liu, Z., Guo, Y., Xue, Y., and Adams, J.M. (2024). Bacterial community network complexity and role of stochasticity decrease during primary succession. *Soil Ecol. Lett.* 6, 230218. <https://doi.org/10.1007/s42832-023-0218-y>.
59. Lei, S., Wang, X., Wang, J., Zhang, L., Liao, L., Liu, G., Wang, G., Song, Z., and Zhang, C. (2024). Effect of aridity on the β -diversity of alpine soil potential diazotrophs: Insights into community assembly and co-occurrence patterns. *mSystems* 9, e0104223. <https://doi.org/10.1128/mSystems.01042-23>.
60. Yuan, H., Li, T., Li, H., Wang, C., Li, L., Lin, X., and Lin, S. (2021). Diversity distribution, driving factors and assembly mechanisms of free-living and particle-associated bacterial communities at a subtropical marginal sea. *Microorganisms* 9, 2445. <https://doi.org/10.3390/microorganisms9122445>.
61. Pearman, J.K., Thomson-Laing, G., Thompson, L., Waters, S., Vander-goes, M.J., Howarth, J.D., Duggan, I.C., Hogg, I.D., and Wood, S.A. (2022). Human access and deterministic processes play a major role in

- structuring planktonic and sedimentary bacterial and eukaryotic communities in lakes. *PeerJ* 10, e14378. <https://doi.org/10.7717/peerj.14378>.
62. Yokoyama, D., and Kikuchi, J. (2023). Inferring microbial community assembly in an urban river basin through geo-multi-omics and phylogenetic bin-based null-model analysis of surface water. *Environ. Res.* 237, 116202. <https://doi.org/10.1016/j.envres.2023.116202>.
 63. Sun, C., Zhang, S., Yang, J., Zhou, H., Cheng, H., Chen, Z., Yu, L., Wang, Y., and Chen, X. (2024). Discrepant assembly processes of prokaryotic communities between the abyssal and hadal sediments in Yap Trench. *Environ. Res.* 241, 117602. <https://doi.org/10.1016/j.envres.2023.117602>.
 64. Canfield, D.E., and Thamdrup, B. (2009). Towards a consistent classification scheme for geochemical environments, or, why we wish the term 'suboxic' would go away. *Geobiology* 7, 385–392. <https://doi.org/10.1111/j.1472-4669.2009.00214.x>.
 65. Xiao, X., Zhang, Y., and Wang, F. (2021). Hydrostatic pressure is the universal key driver of microbial evolution in the deep ocean and beyond. *Environ. Microbiol. Rep.* 13, 68–72. <https://doi.org/10.1111/1758-2229.12915>.
 66. Chattopadhyay, M.K., Raghu, G., Sharma, Y.V., Biju, A.R., Rajasekharan, M.V., and Shivaji, S. (2011). Increase in oxidative stress at low temperature in an Antarctic bacterium. *Curr. Microbiol.* 62, 544–546. <https://doi.org/10.1007/s00284-010-9742-y>.
 67. Parada, A.E., Needham, D.M., and Fuhrman, J.A. (2016). Every base matters: assessing small subunit rRNA primers for marine microbiomes with mock communities, time series and global field samples. *Environ. Microbiol.* 18, 1403–1414. <https://doi.org/10.1111/1462-2920.13023>.
 68. Louca, S., Doebeli, M., and Parfrey, L.W. (2018). Correcting for 16S rRNA gene copy numbers in microbiome surveys remains an unsolved problem. *Microbiome* 6, 41. <https://doi.org/10.1186/s40168-018-0420-9>.
 69. Gao, Z.M., Huang, J.M., Cui, G.J., Li, W.L., Li, J., Wei, Z.F., Chen, J., Xin, Y.Z., Cai, D.S., Zhang, A.Q., and Wang, Y. (2019). *In situ* meta-omic insights into the community compositions and ecological roles of hadal microbes in the Mariana Trench. *Environ. Microbiol.* 21, 4092–4108. <https://doi.org/10.1111/1462-2920.14759>.
 70. Li, Y., Kan, J., Liu, F., Lian, K., Liang, Y., Shao, H., McMinn, A., Wang, H., and Wang, M. (2024). Depth shapes microbiome assembly and network stability in the Mariana Trench. *Microbiol. Spectr.* 12, e0211023. <https://doi.org/10.1128/spectrum.02110-23>.
 71. Jiang, H., Xu, H., Vetter, P.A., Xie, Q., Yu, J., Shang, X., and Yu, L. (2021). Ocean circulation in the Challenger Deep derived from super-deep underwater glider observation. *Geophys. Res. Lett.* 48, GL093169. <https://doi.org/10.1029/2021gl093169>.
 72. van Haren, H., Berndt, C., and Klauke, I. (2017). Ocean mixing in deep-sea trenches: New insights from the Challenger Deep, Mariana Trench. *Deep Sea Research Part I: Oceanographic Research Papers* 129, 1–9. <https://doi.org/10.1016/j.dsr.2017.09.003>.
 73. Peoples, L.M., Kyaw, T.S., Ugalde, J.A., Mullane, K.K., Chastain, R.A., Yayanos, A.A., Kusube, M., Methé, B.A., and Bartlett, D.H. (2020). Distinctive gene and protein characteristics of extremely piezophilic *Colwellia*. *BMC Genomics* 21, 692. <https://doi.org/10.1186/s12864-020-07102-y>.
 74. Scoma, A. (2021). Functional groups in microbial ecology: updated definitions of piezophiles as suggested by hydrostatic pressure dependence on temperature. *ISME J.* 15, 1871–1878. <https://doi.org/10.1038/s41396-021-00930-0>.
 75. Lauro, F.M., and Bartlett, D.H. (2008). Prokaryotic lifestyles in deep sea habitats. *Extremophiles* 12, 15–25. <https://doi.org/10.1007/s00792-007-0110-1>.
 76. Olm, M.R., Brown, C.T., Brooks, B., and Banfield, J.F. (2017). dRep: A tool for fast and accurate genomic comparisons that enables improved genome recovery from metagenomes through de-replication. *ISME J.* 11, 2864–2868. <https://doi.org/10.1038/ismej.2017.126>.
 77. Alneberg, J., Karlsson, C.M.G., Divne, A.-M., Bergin, C., Homa, F., Lindh, M.V., Hugerth, L.W., Ettema, T.J.G., Bertilsson, S., Andersson, A.F., and Pinhassi, J. (2018). Genomes from uncultivated prokaryotes: a comparison of metagenome-assembled and single-amplified genomes. *Microbiome* 6, 173. <https://doi.org/10.1186/s40168-018-0550-0>.
 78. Johnson, J.S., Spakowicz, D.J., Hong, B.Y., Petersen, L.M., Demkowicz, P., Chen, L., Leopold, S.R., Hanson, B.M., Agresta, H.O., Gerstein, M., et al. (2019). Evaluation of 16S rRNA gene sequencing for species and strain-level microbiome analysis. *Nat. Commun.* 10, 5029. <https://doi.org/10.1038/s41467-019-13036-1>.
 79. Pruesse, E., Quast, C., Knittel, K., Fuchs, B.M., Ludwig, W., Peplies, J., and Glöckner, F.O. (2007). SILVA: A comprehensive online resource for quality checked and aligned ribosomal RNA sequence data compatible with ARB. *Nucleic Acids Res.* 35, 7188–7196. <https://doi.org/10.1093/nar/gkm864>.
 80. Bolyen, E., Rideout, J.R., Dillon, M.R., Bokulich, N.A., Abnet, C.C., Al-Ghalith, G.A., Alexander, H., Alm, E.J., Arumugam, M., Asnicar, F., et al. (2019). Reproducible, interactive, scalable and extensible microbiome data science using QIIME 2. *Nat. Biotechnol.* 37, 852–857. <https://doi.org/10.1038/s41587-019-0209-9>.
 81. Robeson, M.S., 2nd, O'Rourke, D.R., Kaehler, B.D., Ziemski, M., Dillon, M.R., Foster, J.T., and Bokulich, N.A. (2021). RESCRIPt: Reproducible sequence taxonomy reference database management. *PLoS Comput. Biol.* 17, e1009581. <https://doi.org/10.1371/journal.pcbi.1009581>.
 82. Martin, M. (2011). Cutadapt removes adapter sequences from high-throughput sequencing reads. *EMBnet. j.* 17, 3. <https://doi.org/10.14806/ej.17.1.200>.
 83. Callahan, B.J., McMurdie, P.J., Rosen, M.J., Han, A.W., Johnson, A.J.A., and Holmes, S.P. (2016). DADA2: High-resolution sample inference from Illumina amplicon data. *Nat. Methods* 13, 581–583. <https://doi.org/10.1038/nmeth.3869>.
 84. Chen, S., Zhou, Y., Chen, Y., and Gu, J. (2018). fastp: an ultra-fast all-in-one FASTQ preprocessor. *Bioinformatics* 34, i884–i890. <https://doi.org/10.1093/bioinformatics/bty560>.
 85. Li, D., Liu, C.-M., Luo, R., Sadakane, K., and Lam, T.-W. (2015). MEGAHIT: an ultra-fast single-node solution for large and complex metagenomics assembly via succinct *de Bruijn* graph. *Bioinformatics* 31, 1674–1676. <https://doi.org/10.1093/bioinformatics/btv033>.
 86. Kang, D.D., Li, F., Kirton, E., Thomas, A., Egan, R., An, H., and Wang, Z. (2019). MetaBAT 2: An adaptive binning algorithm for robust and efficient genome reconstruction from metagenome assemblies. *PeerJ* 7, e7359. <https://doi.org/10.7717/peerj.7359>.
 87. Li, H., and Durbin, R. (2009). Fast and accurate short read alignment with Burrows–Wheeler transform. *Bioinformatics* 25, 1754–1760. <https://doi.org/10.1093/bioinformatics/btp324>.
 88. Chaumeil, P.A., Mussig, A.J., Hugenholtz, P., and Parks, D.H. (2022). GTDB-Tk v2: Memory friendly classification with the genome taxonomy database. *Bioinformatics* 38, 5315–5316. <https://doi.org/10.1093/bioinformatics/btac672>.
 89. Hyatt, D., Chen, G.-L., LoCascio, P.F., Land, M.L., Larimer, F.W., and Hauser, L.J. (2010). Prodigal: Prokaryotic gene recognition and translation initiation site identification. *BMC Bioinformatics* 11, 119. <https://doi.org/10.1186/1471-2105-11-119>.
 90. Queirós, P., Delogu, F., Hickl, O., May, P., and Wilmes, P. (2021). Mantis: Flexible and consensus-driven genome annotation. *GigaScience* 10, giab042. <https://doi.org/10.1093/gigascience/giab042>.
 91. Yu, G. (2020). Using ggtree to visualize data on tree-like structures. *Curr. Protoc. Bioinformatics* 69, e96. <https://doi.org/10.1002/cpbi.96>.
 92. Xu, S., Dai, Z., Guo, P., Fu, X., Liu, S., Zhou, L., Tang, W., Feng, T., Chen, M., Zhan, L., et al. (2021). ggtreeExtra: Compact visualization of richly annotated phylogenetic data. *Mol. Biol. Evol.* 38, 4039–4042. <https://doi.org/10.1093/molbev/msab166>.

93. Oksanen, J., Blanchet, F.G., Kindt, R., Legendre, P., Minchin, P., O'Hara, B., Simpson, G., Solymos, P., Stevens, H., and Wagner, H. (2015). *Vegan: Community Ecology Package*. R Package Version 2.2-1.
94. Wilkinson, L. (2011). ggplot2: elegant graphics for data analysis by WICKHAM, H. *Biometrics* 67, 678–679. <https://doi.org/10.1111/j.1541-0420.2011.01616.x>.
95. R Core Team (2013). *R: A Language and Environment for Statistical Computing* (R Foundation for Statistical Computing).
96. Pedersen, T.L. (2021). *ggraph: An implementation of grammar of graphics for graphs and networks*. *ggraph*.
97. Csardi, G., and Nepusz, T. (2005). The igraph software package for complex network research. *InterJournal. Complex Syst.* 1695, 1–9.
98. Xiao, N., Zhou, A., Kempfer, M.L., Zhou, B.Y., Shi, Z.J., Yuan, M., Guo, X., Wu, L., Ning, D., Van Nostrand, J., et al. (2022). Disentangling direct from indirect relationships in association networks. *Proc. Natl. Acad. Sci. USA* 119, e2109995119.
99. Vieira-Silva, S., and Rocha, E.P.C. (2010). The systemic imprint of growth and its uses in ecological (meta) genomics. *PLoS Genet.* 6, e1000808. <https://doi.org/10.1371/journal.pgen.1000808>.
100. Walters, W., Hyde Embriette, R., Berg-Lyons, D., Ackermann, G., Humphrey, G., Parada, A., Gilbert Jack, A., Jansson Janet, K., Caporaso, J.G., Fuhrman Jed, A., et al. (2016). Improved bacterial 16S rRNA gene (V4 and V4-5) and Fungal Internal Transcribed Spacer Marker Gene Primers for Microbial Community Surveys. *mSystems* 1, e00009-00015. <https://doi.org/10.1128/msystems.00009-15>.
101. Wang, J., Zhang, Q., Wu, G., Zhang, C., Zhang, M., and Zhao, L. (2018). Minimizing spurious features in 16S rRNA gene amplicon sequencing. *PeerJ Prepr.* 6, v26871. <https://doi.org/10.7287/peerj.preprints.26872>.
102. Weiss, S., Xu, Z.Z., Peddada, S., Amir, A., Bittinger, K., Gonzalez, A., Lozupone, C., Zaneveld, J.R., Vázquez-Baeza, Y., Birmingham, A., et al. (2017). Normalization and microbial differential abundance strategies depend upon data characteristics. *Microbiome* 5, 27. <https://doi.org/10.1186/s40168-017-0237-y>.
103. McDonald, D., Clemente, J.C., Kuczynski, J., Rideout, J.R., Stombaugh, J., Wendel, D., Wilke, A., Huse, S., Hufnagle, J., Meyer, F., et al. (2012). The biological observation matrix (BIOM) format or: how I learned to stop worrying and love the ome-ome. *GigaScience* 1, 7. <https://doi.org/10.1186/2047-217x-1-7>.
104. McKinney, W. (2010). Data structures for statistical computing in Python. *Proceedings of the Python in Science Conference*, 56–61.
105. Bokulich, N.A., Kaehler, B.D., Rideout, J.R., Dillon, M., Bolyen, E., Knight, R., Huttley, G.A., and Gregory Caporaso, J. (2018). Optimizing taxonomic classification of marker-gene amplicon sequences with QIIME 2's q2-feature-classifier plugin. *Microbiome* 6, 90. <https://doi.org/10.1186/s40168-018-0470-z>.
106. Pedregosa, F., Varoquaux, G., Gramfort, A., Michel, V., Thirion, B., Grisel, O., Blondel, M., Prettenhofer, P., Weiss, R., and Dubourg, V. (2011). Scikit-learn: Machine learning in Python. *J. Mach. Learn. Res.* 12, 2825–2830. <https://doi.org/10.5555/1953048.2078195>.
107. Rognes, T., Flouri, T., Nichols, B., Quince, C., and Mahé, F. (2016). VSEARCH: A versatile open source tool for metagenomics. *PeerJ* 4, e2584. <https://doi.org/10.7717/peerj.2584>.
108. Ostertagová, E., Ostertag, O., and Kováč, J. (2014). Methodology and application of the Kruskal-Wallis test. *Appl. Mech. Mater.* 677, 115–120.
109. Deng, Y., Jiang, Y.H., Yang, Y., He, Z., Luo, F., and Zhou, J. (2012). Molecular ecological network analyses. *BMC Bioinformatics* 13, 113. <https://doi.org/10.1186/1471-2105-13-113>.
110. Zhou, J., Deng, Y., Luo, F., He, Z., Tu, Q., and Zhi, X. (2010). Functional molecular ecological networks. *mBio* 1, e00169-10. <https://doi.org/10.1128/mbio.00169-10>.
111. Zhou, J., Deng, Y., Luo, F., He, Z., and Yang, Y. (2011). Phylogenetic molecular ecological network of soil microbial communities in response to elevated CO₂. *mBio* 2, e00122-11. <https://doi.org/10.1128/mbio.00122-11>.

STAR★METHODS

KEY RESOURCES TABLE

REAGENT or RESOURCE	SOURCE	IDENTIFIER
Biological samples		
Sediment samples	Collected from the Mariana Trench, the Yap Trench and the Philippine Basin	MEER
Critical commercial assays		
MGIEasy Environmental Microbiome DNA Extraction Kit	MGI-Tech, China	Cat#940-001731-00
MGIEasy Fast FS DNA Library Prep Set	MGI-Tech, China	Cat#940-000030-00
Deposited data		
Raw data	This paper	CNSA: CNP0004890
Raw data	This paper	NODE: OEP004067
Shotgun metagenome-derived species-level representative genomes	This paper	eLMSG: LMSG_G000037053.1 – LMSG_G000044616.1
Source code for quality control, assembly, binning, classification, and abundance profiling	This paper	https://github.com/meer-trench/genome_catalogue
Source code for ecological analyses	This paper	https://doi.org/10.5281/zenodo.13317475
Ocean Microbiomics Database	Paoli et al. ³⁰	https://microbiomics.io/ocean/
GTDB database release 220	Parks et al. ⁴⁹	https://gtdb.ecogenomic.org/
SILVA database version 138	Pruesse et al. ⁷⁹	https://www.arb-silva.de/
Greengenes2 database release 2022.10	McDonald et al. ⁵²	https://ftp.microbio.me/greengenes_release/2022.10/
Oligonucleotides		
515F (Parada), Forward	5'-GTGYCAGCMGCCGCGTAA-3'	N/A
806R (Apprill), Reverse	5'-GGACTACNVGGGTWTCTAAT-3'	N/A
Software and algorithms		
QIMME2	Bolyen et al. ⁸⁰	https://github.com/qiime2
RESCRIPt (2024.10.0.dev0+7.g3c179ca)	Robeson et al. ⁸¹	https://github.com/bokulich-lab/RESCRIPt
Cutadapt	Martin et al. ⁸²	https://cutadapt.readthedocs.io/en/stable/
DADA2	Callahan et al. ⁸³	https://github.com/benjjneb/dada2
fastp (v0.23.2)	Chen et al. ⁸⁴	https://github.com/OpenGene/fastp
MEGAHIT (v1.2.9)	Li et al. ⁸⁵	https://github.com/voutcn/megahit
MetaBAT2 (v2.12.1)	Kang et al. ⁸⁶	https://bitbucket.org/berkeleylab/metabat
BWA (v0.7.17-r1188)	Li et al. ⁸⁷	https://github.com/lh3/bwa
dRep (v3.4.0)	Olm et al. ⁷⁶	https://github.com/MrOlm/drep
CoverM (v0.7.0)	N/A	https://github.com/wwood/CoverM
GTDB-Tk (v2.4.0)	Chaumeil et al. ⁸⁸	https://github.com/ECogenomics/GTDBTk
Prodigal	Hyatt et al. ⁸⁹	https://github.com/hyatt/Prodigal
Mantis	Queirós et al. ⁹⁰	https://github.com/PedroMTQ/mantis
R (v4.1.0)	R Project	https://www.r-project.org/
R Studio Server v2023.12.1.402	Posit®	https://posit.co/products/open-source/rstudio-server/
ggtree (v3.10.1)	Yu et al. ⁹¹	https://github.com/YuLab-SMU/ggtree
ggtreeExtra (v1.12.0)	Xu et al. ⁹²	https://github.com/YuLab-SMU/ggtreeExtra
vegan (v2.6-4)	Oksanen et al. ⁹³	https://github.com/vegandevs/vegan

(Continued on next page)

Continued

REAGENT or RESOURCE	SOURCE	IDENTIFIER
ggplot2 (v3.5.1)	Wilkinson et al. ⁹⁴	https://github.com/tidyverse/ggplot2
stats (v4.1.3)	R Core Team ⁹⁵	https://www.r-project.org
iCAMP (v1.5.12)	Ning et al. ²³	https://github.com/DaliangNing/iCAMP1
ggraph (v2.2.1)	Pedersen et al. ⁹⁶	https://github.com/thomasp85/ggraph
igraph (v2.0.3)	Csardi et al. ⁹⁷	https://github.com/igraph/igraph
MENA	Xiao et al. ⁹⁸	http://ieg4.rccc.ou.edu/mena/login.cgi
Growthpred (v1.07)	Vieira-Silva et al. ⁹⁹	http://mobyle.pasteur.fr/cgi-bin/portal.py?form=growthpred
Other		
Typical deep-sea sediment metagenomes and reported hadal metagenomes	BioProject	Table S2

EXPERIMENTAL MODEL AND STUDY PARTICIPANT DETAILS

No experimental models nor human participants were included in this study. Samples used in this study were directly collected from natural oceanic environments using the HOV *Fendouzhe* and equipments onboard. No culturing of microbe strains, cell lines, nor primary cell cultures has been conducted.

METHOD DETAILS

Sample collection and DNA extraction

We used HOV *Fendouzhe* to collect sediment samples via push core plastic tubes (typically 50 cm in length), and the samples were subsequently transferred back to the ship and sliced vertically almost every two centimeters. The samples were subsequently stored in a refrigerator until further analysis. To extract microbial DNA, we thawed 0.5 g sediment samples and used China National GenBank commercial kits (MGI Easy Environmental Microbiome DNA Extraction Kit, Item No. 940-001731-00, MGI-Tech, China). We performed up to three additional extractions for the samples that yielded low amounts of DNA, and the DNA derived from the same samples was combined and concentrated.

16S rRNA gene amplicon sequencing and analysis

The V4 region of the 16S rRNA gene was amplified via the forward-barcoded primer pair 515F (Parada)-806R (Apprill),¹⁰⁰ Fwd: GTGYCAGCMGCCGCGGTAA; Rev: GGACTACNVGGGTWCTAAT. The libraries were prepared and sequenced by Biomarker Biotechnology Co., Ltd. (Beijing, China) via the Illumina NovaSeq 6000 sequencing system (Illumina, Santiago, CA, USA) for 2*250 bp paired-end sequencing. The sequencing reads were analyzed via the QIIME2 platform (2024.5 Amplicon Distribution).⁸⁰ Briefly, the adaptors and primers were trimmed with Cutadapt.⁸² Next, the paired-end reads were merged and denoised into amplicon sequence variance (ASVs) via DADA2.⁸³ ASVs with < 7 reads were considered unreliable and thus were filtered out as described previously.¹⁰¹ The final ASV table was rearranged to retain 50,000 reads per sample to avoid bias from uneven sequencing depths.^{102–104} Next, the ASVs were classified via sklearn against the training set from three databases: the SILVA database version 138, the SSU sequences from the GTDB database release 220, and the Greengenes2 database release 2022.10.^{49,51,52,79,105–107} RESCRIPt was used to fetch the reference SSU sequences and build ASV-specific taxonomy classifier from GTDB database.⁸¹ To optimize the taxonomic classification accuracy, the reference sequences from the three databases were first trimmed to the V4 region via the same PCR primer pair. The ASVs were directly mapping to the three databases via the species-level 97% identity threshold by VSEARCH (v2.22.1).¹⁰⁷

Metagenomic sequencing, binning and annotation

To construct libraries, we used high-efficiency library preparation kits (MGI Easy Fast FS DNA Library Prep Set, Item No. 940-000030-00, MGI-Tech, China). Sequencing was conducted on the DNBSEQ-T series machines to obtain 150 bp of read-length raw reads. The fastp (v0.23.2)⁸⁴ was used to perform quality control and adaptor removal for the raw sequencing data. The clean reads were subsequently assembled via MEGAHIT (v1.2.9),⁸⁵ and the assembled contigs per sample were subjected to contig binning via MetaBAT2 (v2.12.1).⁸⁶ The clean reads from each individual sample were aligned to its own assembly and the assemblies of 99 other randomly picked samples via BWA-MEM (v0.7.17-r1188),⁸⁷ resulting in a depth matrix for each sample spanning 100 samples.

The metagenome-assembled genomes (MAGs) with completeness $\geq 50\%$ and contamination $\leq 10\%$ were filtered and subjected to two rounds of dereplication via dRep (v3.4.0).⁷⁶ The average nucleotide identity (ANI) threshold was first set at 0.99 then 0.95 to obtain the species-level representative SRGs. The coverM (v0.7.0) was used to calculate the relative abundance of these SRGs with the RPKM (Reads Per Kilobase Million) method (<https://github.com/wwood/CoverM>). This method inherently accounts for

differences in genome size and sequencing depth, which ensures accurate abundance estimates despite varying completeness of SRGs. Taxonomic annotation of the 7,564 species SRGs was subsequently performed against the GTDB database release 220.⁴⁹ The results were subsequently utilized to construct phylogenetic trees for both archaea and bacteria via the R packages “ggtree” (v3.10.1)⁹¹ and “ggtreeExtra” (v1.12.0).⁹² The GTDB-Tk (v2.4.0)⁸⁸ `infer_ranks` module was subsequently employed to calculate the relative evolution divergence (RED) value.⁵⁰

The genes in SRGs were predicted with Prodigal in “single” mode.⁸⁹ Then they were subsequently collected and annotated with the tool Mantis,⁹⁰ and KEGG ortholog information of each SRG was collected.

Biogeographic distribution analysis

The alpha diversity (Shannon index, phylogenetic diversity and Simpson index) and beta diversity (Bray–Curtis index) were calculated via the “vegan” package (v2.6-4)⁹³ and visualized via the “ggplot2” package (v3.5.1)⁹⁴ in R (v4.1.0) within the Rstudio Server v2023.12.1.402. The difference in alpha diversity was calculated via the Kruskal–Wallis test¹⁰⁸ and the significance between each group was further calculated using pairwise Wilcoxon rank-sum test via the “stats” package (v4.1.0).⁹⁵ NMDS, PCoA and permutational multivariate analysis of variance (PERMANOVA) were conducted via the “vegan” package (v2.6-4).⁹³

Microbial community assembly calculation

We calculated the ecological driving forces of the microbial community by employing the R package “iCAMP” (v1.5.12)²³ using the abundance of 3270 good-quality SRGs (completeness > 75%, contamination < 10%, representing 56% of total SRG abundance). The relative abundance of SRGs and their phylogenetic tree were used as inputs, with a set of parameters: `ds` (phylogenetic distance cutoff) = 0.2, `bin.size.limit` (minimal requirement of bin size) = 48, `rand.time` = 200, `sig.index` (the index for null model significant test) = “Confidence”, `detail.null` = False. In addition, the top 50,000 ASVs accounting for 90% relative abundance were also selected to conduct iCAMP with `bin.size.limit` = 480 and `rand.time` = 100.

Molecular ecological network construction and analyses

We used the molecular ecological network analysis pipeline (MENA) (<http://ieg4.rccc.ou.edu/mena/login.cgi>), which combines the random matrix theory (RMT)-based network method and the iDIRECT framework⁹⁸ to construct microbial networks based on the relative abundance of good-quality SRGs. The automatically threshold was set based on the transition of Gaussian orthogonal ensemble statistics and Poisson distributions and noise removal.^{109–111} Furthermore, we used the R packages “ggraph” (v2.2.1)⁹⁶ and “igraph” (v2.0.3)⁹⁷ to visualize networks for better comparison with the “nicely” layout.

Genomic and physiological trait prediction of SRGs

To detect genome traits, we used Growthpred (v1.07)⁹⁹ to predict the optimal growth temperature (OGT) and mean generation time (MGT) of good-quality SRGs. To detect the potential linkages between indices, we used a linear mixed-effects model of R package “stats” (v4.1.0)⁹⁵ to predict the correlations between genomics traits (genome size, GC content, OGT, MGT) and the relative importance of ecological processes.

Supplemental figures

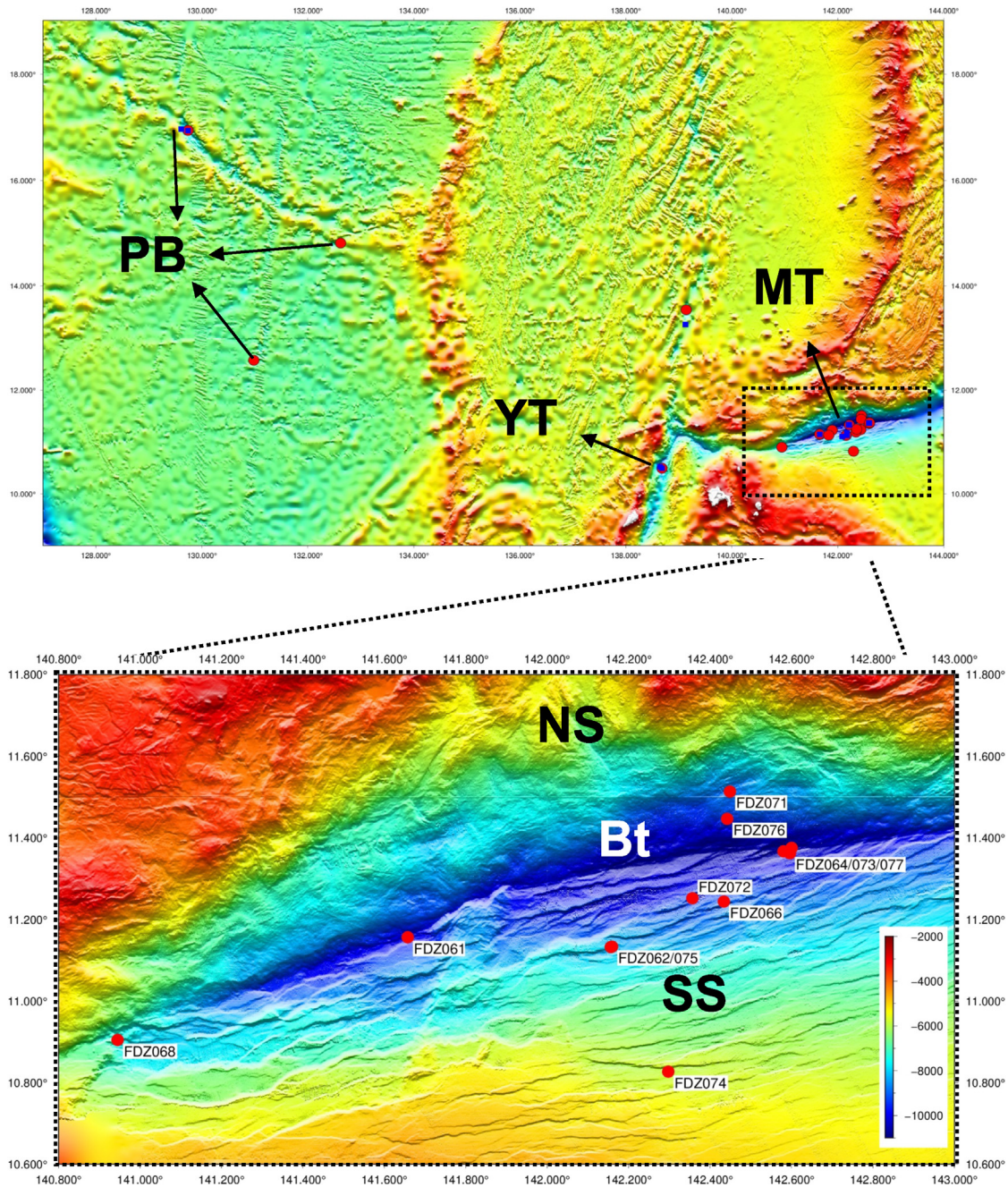


Figure S1. Sampling sites of sediment samples in the hadal zones, related to Figure 1

The HOV *Fendouzhe* was used to collect sediment samples from the Philippine Basin (PB), Yap Trench (YT), and Mariana Trench (MT). Sampling in the MT encompassed three representative topographical regions: the bottom (Bt), the northern slope (NS), and the southern slope (SS).

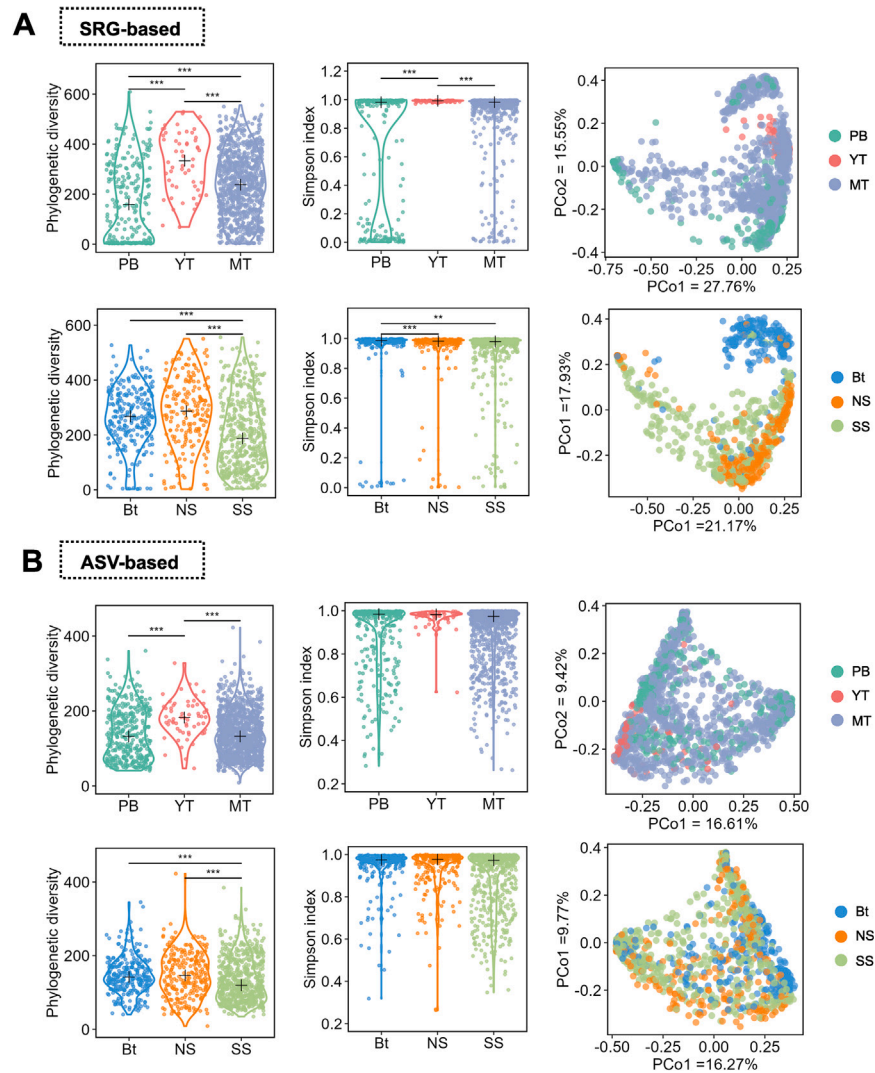


Figure S2. The diversity of the microbiome in the hadal zones, related to Figure 2

(A) SRG-based microbial phylogenetic diversity, Simpson index, and principal coordinates analysis (PCoA) based on the Bray-Curtis distance in the Philippine Basin (PB), Yap Trench (YT) and Mariana Trench (MT) and different topographical areas: the bottom (Bt), the northern slope (NS), and the southern slope (SS) within the MT.

(B) 16S rRNA gene-ASV-based microbial phylogenetic diversity, Simpson index, and PCoA based on the Bray-Curtis distance in the PB, YT, and MT, as well as Bt, NS, and SS within the MT. The black cross of violin chart represented the median value. The asterisks indicated significant differences using pairwise Wilcoxon rank-sum test: *** $p < 0.001$, ** $p < 0.01$, * $p < 0.05$.

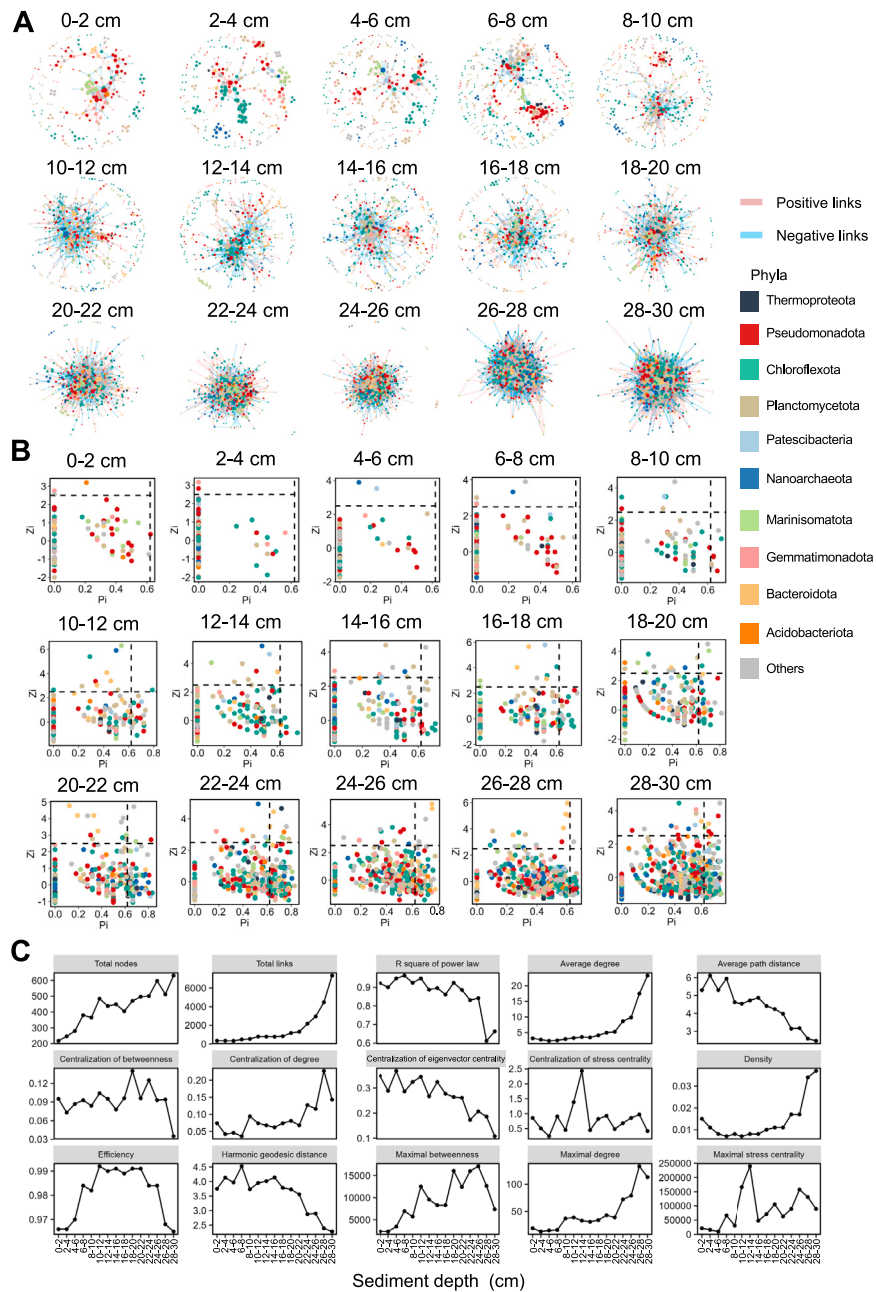
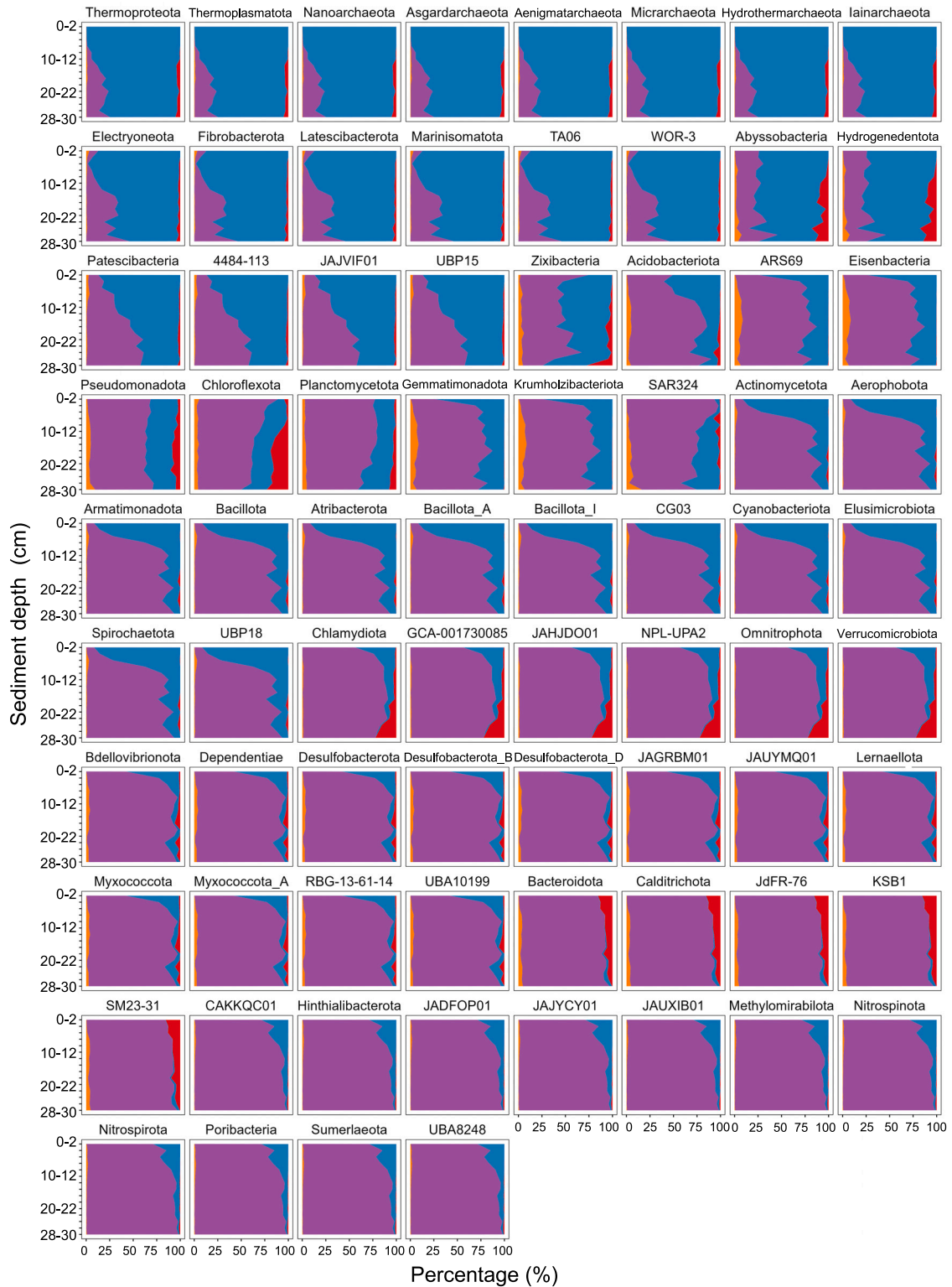


Figure S3. The networks along the sediment depth gradient (0–30 cm) within the Mariana Trench, related to Figure 4

(A) The network graph of the different sediment depths with a “nice” layout. The nodes (SRGs) were colored by the top 10 phyla.

(B) Zi-Pi plot of networks from different sediment depths demonstrating the distribution of SRGs based on module-based topological roles. Zi, within-module connectivity; Pi, among-module connectivity.

(C) The topological parameters of networks of different sediment layers (0–30 cm).



HeS HoS DL DR HD

(legend on next page)

Figure S4. The relative importance of ecological processes of microbial phyla along the sediment depth gradient (0–30 cm) within the Mariana Trench, related to [Figure 4](#)
HeS, heterogeneous selection; HoS, homogeneous selection; DL, dispersal limitation; DR, drift; HD, homogenizing dispersal.

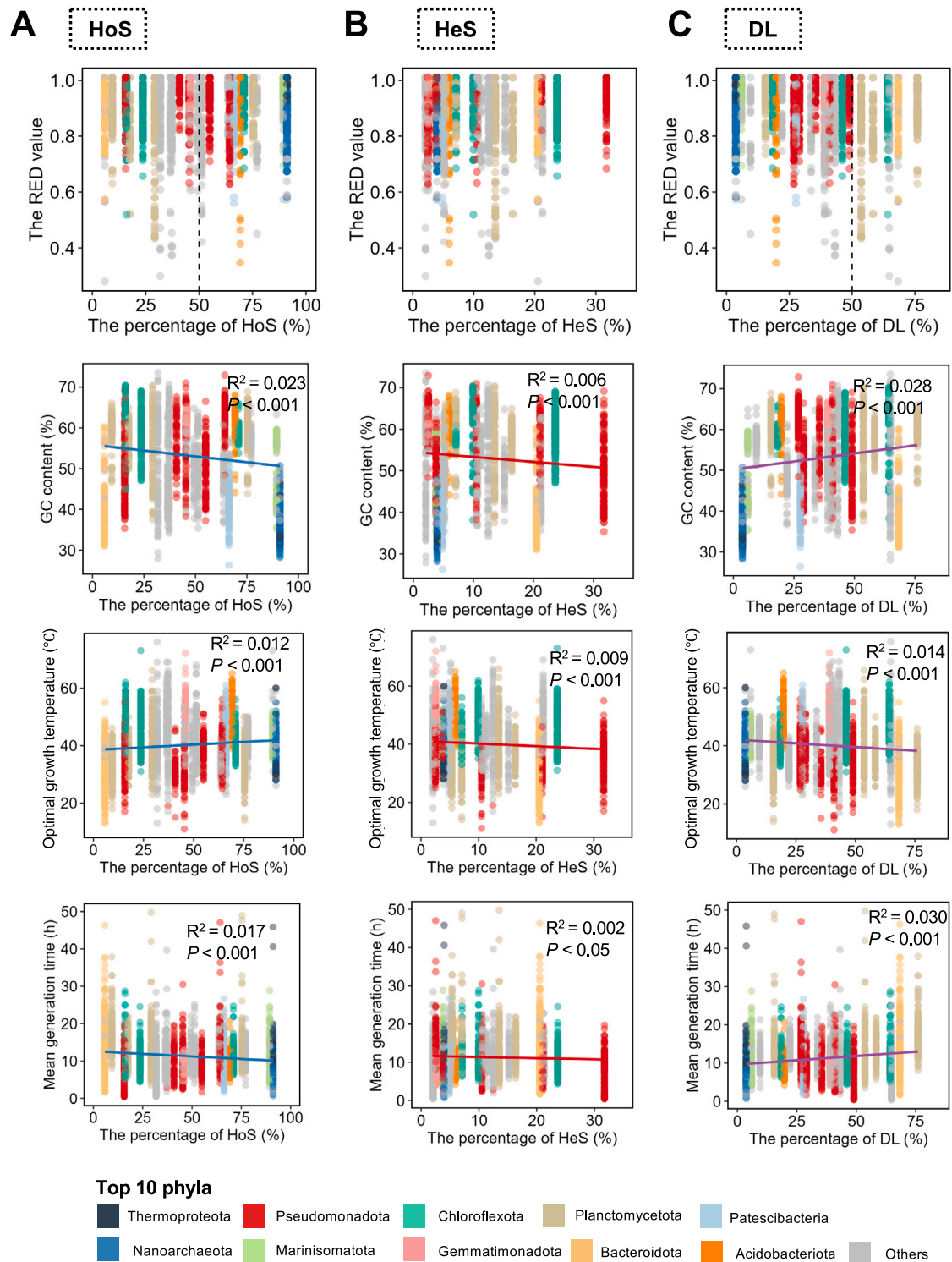


Figure S5. The correlation of the percentage of main driving forces and genomic features of SRGs, related to Figure 5

The correlation of the relative importance of homogeneous selection (A), heterogeneous selection (B), and dispersal limitation (C) and the relative evolutionary divergence (RED) value, GC content, the optimal growth temperature, and the mean generation time of SRGs.